Interaction of panel flutter with inviscid boundary layer instability in supersonic flow

Vasily Vedeneev†

Faculty of Mechanics and Mathematics, Lomonosov Moscow State University, Moscow, 119991, Russia

We investigate the stability of an elastic plate in supersonic gas flow. This problem has been studied in many papers regarding panel flutter, where uniform flow is usually considered. In this paper, we take the boundary layer on the plate into account and investigate its influence on plate stability. Three problem formulations are studied. First, we investigate the stability of travelling waves in an infinite-length plate. Second, the nature of the instability (absolute or convective instability) is examined. Finally, by using solutions of the first two problems, instability of a long finite-length plate is studied by using Kulikovskii's global instability criterion. The following results are obtained. All the eigenmodes of a finite-length plate are split into two types, which we call subsonic and supersonic. The influence of the boundary layer on these eigenmodes can be of two kinds. First, for a generalized convex boundary layer profile (typical for accelerating flow), supersonic eigenmodes are stabilized by the boundary layer, whereas subsonic disturbances are destabilized. Second, for a profile with a generalized inflection point (typical for constant and decelerating flows), supersonic eigenmodes are destabilized in a thin boundary layer and stabilized in a thick layer; subsonic eigenmodes are damped. The correspondence between the influence of the boundary layer on panel flutter and the stability of the boundary layer over a rigid wall is established. Examples of stable boundary layer profiles of both types are given.

Key words: flow–structure interactions, boundary layer stability, absolute/convective instability

1. Introduction

The classical stability theory of shear flows deals with fluid flows over rigid surfaces. Many different ways to control laminar–turbulent transition have been studied, such as cooling or heating of the surface, boundary layer suction or blowing, and surface porosity. Following Kramer (1960), a series of papers is devoted to the investigation of boundary layer stability over compliant surfaces. Besides earlier studies reviewed in the fundamental work by Carpenter & Garrad (1985, 1986), we mention papers by Savenkov (1995), Reutov & Rybushkina (1998), Lingwood & Peake (1999), Miles (2001), Wiplier & Ehrenstein (2001) and Boiko & Kulik (2012). It has been shown that elastic and viscous properties of the surface can significantly change the shape of the neutral stability curve and can change the character of instability from convective to absolute. Also, in addition to inviscid inflection-point instability and

† Email address for correspondence: vasily@vedeneev.ru

viscous Tollmien–Schlichting instability, a series of new instability types appears due to flexibility of the surface (Carpenter & Garrad 1985, 1986).

The stability of compressible shear flows, and especially of supersonic flows over a compliant wall, has been much less studied. In supersonic flows over a compliant wall, one more instability type appears, namely, panel flutter (Bolotin 1963; Dowell 1974). It is dangerous not because of flow transition to turbulence, but primarily because of high-amplitude vibrations of the wall structure. This phenomenon is well known in aviation and has been studied in numerous papers since the 1950s. Until recent years, only one panel flutter type, namely, coupled-mode flutter, had been studied. It occurs due to the coupling of two plate eigenmodes through gas flow. In the case of low supersonic flow speeds, another type of flutter exists, namely, single-mode flutter. Even though this type of flutter was discovered in the 1960s (Dowell 1974), it is still viewed by some as being non-physical, only appearing in calculations due to insufficient accuracy in numerical studies. Recently, however, Vedeneev (2005) analytically proved that this type of flutter does indeed exist; it has subsequently been observed in experiments (Vedeneev *et al.* 2010) and studied numerically (Vedeneev 2012).

The overwhelming majority of investigators of panel flutter did not take the boundary layer into account and considered uniform velocity and temperature profile. In a few papers where the influence of the boundary layer was numerically studied (Dowell 1971, 1973; Hashimoto, Aoyama & Nakamura 2009), a particular velocity profile was considered, namely, the $(1/7)$th power velocity law. The reason is that those studies were devoted to the modelling of experiments by Muhlstein, Gaspers & Riddle (1968) and Gaspers, Muhlstein & Petroff (1970). The same boundary layer profile was studied by Miles (1959). Those studies showed that the boundary layer of this particular profile can decrease the growth rate of unstable eigenmodes or even fully suppress instability. However, in flows over flight vehicles at different flight conditions and for different skin panel locations, boundary layer profiles over panels can differ significantly. In this paper, we analytically study the influence of the arbitrary boundary layer profile on panel flutter and the interaction between flutter and inflection-point instability of the layer.

The paper is organized as follows. First, in §2, we state the problem and discuss the assumptions used. In §3, we derive the dispersion relation for travelling waves in an infinite-length plate subjected to a flow. In §§4 and 5 we investigate the roots of the dispersion relation and the analysis of the stability of an infinite-length plate. In §6, we investigate the stability of a plate that has a long but finite length so that Kulikovskii's asymptotic instability criterion can be used (Kulikovskii 1966*a*). Finally, in §7, we summarize the results of the paper.

2. Formulation of the problem

We investigate the stability of an elastic plate stretched by an isotropic in-plane force. One side of the plate is exposed to shear gas flow; the other side experiences constant pressure equal to an undisturbed pressure of the flow so that the undisturbed state of the plate is flat. The plate is either infinite in all directions or has a shape of a strip, which is mounted into an infinite rigid plane (figure 1). The flow has a boundary layer over the plate surface with given velocity and temperature profiles $u_0(z)$ and $T_0(z)$, respectively. It is assumed that they are governed by the flow conditions over the flight vehicle, whose single panel is represented by the plate considered.

The problem is investigated in a two-dimensional formulation; also, we neglect the growth of the boundary layer so that the unperturbed flow does not depend on x. This
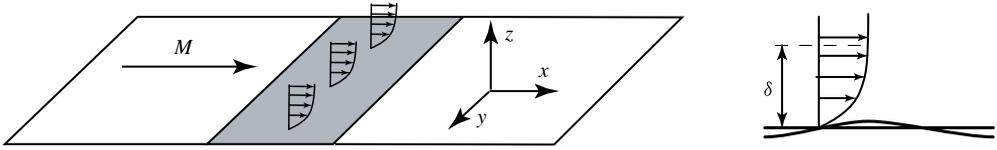
FIGURE 1. Gas flow over elastic plate.

admits perturbations of a travelling wave type, where all variables are proportional to $e^{i(kx-\omega t)}$. We will first investigate the travelling waves themselves and, second, the general solutions constructed as a superposition of travelling waves: wave packets for an infinite plate and Kulikovskii's natural modes for a large finite plate. All variables are assumed to be non-dimensional, with the speed of sound and temperature of the flow outside the boundary layer taken as the velocity and temperature scales, the plate thickness as the length scale, and plate material density as the density scale.

The plate is governed by Kirchhoff–Love small deflection plate theory. In a dimensionless form, the plate equation is as follows:

$$D\frac{\partial^4 w}{\partial x^4} - M_w^2 \frac{\partial^2 w}{\partial x^2} + \frac{\partial^2 w}{\partial t^2} + p(x, 0, t) = 0, \tag{2.1}$$

where $w(x, t)$ is the plate deflection, D is the dimensionless plate stiffness, M_w is the square root of the dimensionless in-plane tension force, and $p(x, z, t)$ is the flow pressure disturbance generated by the plate, which is hence a function of w.

If the plate is infinite, then the only boundary condition that must be satisfied by the deflection is finiteness, i.e. $w(x)$ is limited as $x \to \pm\infty$. If the plate has a finite length L, then two boundary conditions must be satisfied at each plate edge, $x = -L/2$ and $x = L/2$. For example, these could be clamping or pinning boundary conditions.

The flow is assumed to be laminar; the Reynolds number $Re \to \infty$. This means that small perturbations of the flow are governed by the inviscid Rayleigh equation, while viscosity is essential only in the formation of the steady boundary layer as non-uniform distribution of velocity and temperature. Let us discuss these assumptions. First, despite the fact that in supersonic flows turbulent boundary layers are observed more often, laminarity is also possible up to $Re \sim 10^5$ for the Reynolds number based on boundary layer thickness. This value is large enough to neglect viscosity in equations for perturbations (unless the wavenumber is extremely small). Laminar supersonic boundary layers are observed in accelerating flows and uniform flows with the cooling of the plate surface or gas suction (Gaponov & Maslov 1980, chap. 5). In the other case, when the boundary layer is turbulent but typical pulsation frequencies are much higher than the frequency of growing plate oscillations, laminar flow equations can be used in the first approximation, with Reynolds-averaged velocity and temperature profiles taken as steady flow profiles.

Second, solutions of the viscous problem tend to solutions of the Rayleigh equation as $Re \to \infty$ only in a sector of the complex z plane with angle $4\pi/3$ and vertex at $z = z_c$ (figure 2). Here, z_c is the critical point, $u_0(z_c) = c$, and $c = \omega/k$ is the phase speed (Drazin & Reid 2004). In the shaded regions, solutions of the viscous problem are of the WKB type, that is, velocity perturbation $v(z) \sim g(z)\exp(\sqrt{iRe}f(z))$. This leads to Lin's rule for the integration path: if $\text{Im}\, z_c \leqslant 0$ and the WKB region contains a segment of the real ray $z \geqslant 0$, not including the point $z = 0$, then inviscid solutions can be analytically continued from one boundary ($z = 0$) to the other ($z = +\infty$) along a path that must leave the real axis z and pass below the critical point z_c. If the real
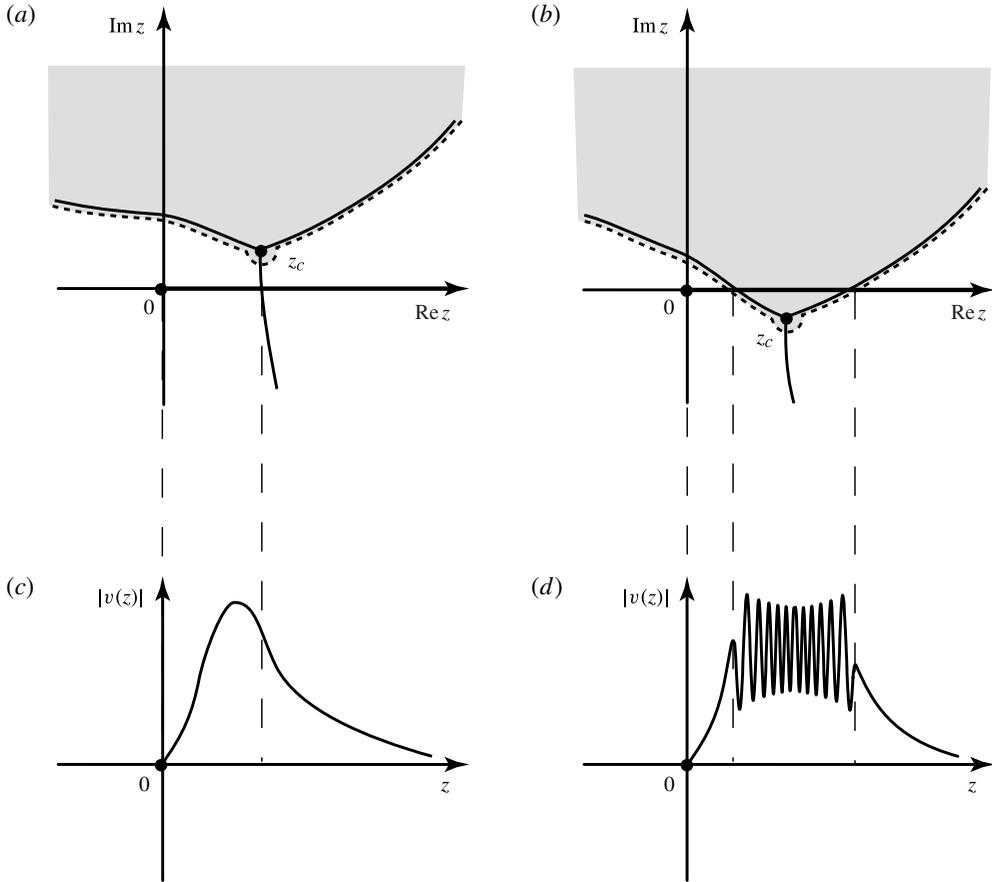
FIGURE 2. (a,b) Stokes lines and WKB regions (shaded) for z_c lying (a) above, (b) below the real axis. (c,d) Apparent behaviour of disturbances at real z.

ray $z \geqslant 0$ does not intersect the WKB region (for example, $\mathrm{Im}\, z_c > 0$), then inviscid solutions can be analytically continued along the ray. However, if the point $z = 0$ lies in the WKB region, then inviscid approximation is not applicable, because it is impossible to satisfy boundary conditions at $z = 0$. We will assume that $u_0'(z) > 0$ throughout the boundary layer, so that for z_c lying in a neighbourhood of the real ray $z \geqslant 0$, it follows that $\mathrm{sign}\,\mathrm{Im}\, z_c = \mathrm{sign}\,\mathrm{Im}\, c$.

Keeping these limitations of the model in mind, we can now proceed to equations. Let $v(z)\mathrm{e}^{\mathrm{i}(kx-\omega t)}$ and $p(z)\mathrm{e}^{\mathrm{i}(kx-\omega t)}$ be the perturbations of vertical velocity component and pressure. Then the compressible Rayleigh equation (Lees & Lin 1946) takes the following form:

$$\frac{\mathrm{d}}{\mathrm{d}z}\left(\frac{(u_0 - c)\,\mathrm{d}v/\mathrm{d}z - v\,\mathrm{d}u_0/\mathrm{d}z}{T_0 - (u_0 - c)^2}\right) - \frac{1}{T_0}k^2(u_0 - c)v = 0. \tag{2.2}$$

The amplitude of pressure perturbation is expressed in terms of $v(z)$ as follows:

$$p(z) = \frac{\mu}{\mathrm{i}k}\frac{(u_0 - c)\,\mathrm{d}v/\mathrm{d}z - v\,\mathrm{d}u_0/\mathrm{d}z}{T_0 - (u_0 - c)^2}, \tag{2.3}$$

where μ is the dimensionless density of the flow outside the boundary layer.

Consider boundary conditions for the Rayleigh equation. First, at the plate surface $z = 0$, we assign the condition of impenetrability along the plate bent into the shape of a travelling wave: $w(x) = e^{i(kx - \omega t)}$. The second boundary condition is the radiation condition as $z \rightarrow +\infty$. We apply it at the outer boundary of the boundary layer $z = \delta$, where δ is the dimensionless boundary layer thickness, as follows. Assume that for $z > \delta$, the flow is uniform, $u_0 \equiv M_\infty$ is the Mach number outside the boundary layer, and $T_0 \equiv 1$. Then for $z > \delta$, Rayleigh equation (2.2) is reduced to an equation with constant coefficients, whose solution is $v(z) = Ce^{\gamma z}$, $\gamma = -\sqrt{k^2 - (M_\infty k - \omega)^2}$. The radiation condition as $z \rightarrow +\infty$ yields a particular square root branch, namely,

$$\mathrm{Re}\,\gamma < 0 \tag{2.4}$$

for $\mathrm{Im}\,\omega \gg 1$. This exponential solution outside the boundary layer must be matched to the solution inside the boundary layer. Thus, the boundary conditions finally take the following form:

$$v = -\mathrm{i}\omega \quad (z = 0), \qquad \frac{1}{v}\frac{\mathrm{d}v}{\mathrm{d}z} = \gamma \quad (z = \delta). \tag{2.5}$$

Hereafter, we assume that the parameter μ (which is the density of the flow outside the boundary layer relative to the plate material density) is small, and use asymptotic expansions as $\mu \rightarrow 0$ wherever possible. In industrial applications, the order of μ is typically in the range 10^{-5}–10^{-3}.

3. Dispersion relation for an infinite plate in a gas flow

In this section, we assume that the plate is infinite and consider travelling wave disturbances: $w(x, t) = e^{i(kx - \omega t)}$. We derive the dispersion relation that connects wavenumber k and frequency ω in the following manner. First, we solve Rayleigh equation (2.2) with boundary conditions (2.5). Second, we calculate disturbance of pressure (2.3) acting on the plate surface. Finally, we substitute the pressure disturbance into the plate equation (2.1) and obtain the dispersion relation.

Note that the Rayleigh equation can have two singularities (Lees & Lin 1946; Lin 1966). The first one is the critical point z_c, where $u_0(z_c) = c$. It leads to the singularity of the solution that will be discussed below. The other one is the point where $T_0(z) - (u_0(z) - c)^2 = 0$, which means that the phase speed of the wave is equal to the local speed of sound. This singularity is removable.

The solution of the Rayleigh equation can be constructed in the form of a convergent series in k^2, known as the Heisenberg expansion (Lees & Lin 1946; Drazin & Reid 2004). In industrial applications related to flutter, wavelengths $\lambda = 2\pi/k$ of practical interest are much larger than the boundary layer thickness δ. Therefore, hereafter in the paper, we assume that $|k|$ is small, namely, $|k| \ll 1/\delta$, and keep only the first term of the series. This is equivalent to neglecting the second term of the order of k^2 in (2.2):

$$\frac{\mathrm{d}}{\mathrm{d}z}\left(\frac{(u_0 - c)\,\mathrm{d}v/\mathrm{d}z - v\,\mathrm{d}u_0/\mathrm{d}z}{T_0 - (u_0 - c)^2}\right) = 0. \tag{3.1}$$

This equation is easily solved, and its general solution is

$$v(z) = \left(c_1\left(\int_0^z \frac{T_0(\zeta)\,\mathrm{d}\zeta}{(u_0(\zeta) - c)^2} - z\right) + c_2\right)(u_0(z) - c). \tag{3.2}$$

Substitution into (2.3) yields the pressure perturbation

$$p(z) \equiv \frac{c_1 \mu}{\mathrm{i}k}. \tag{3.3}$$

It is clearly seen that (3.2) has a singularity at the critical point that is not removable in inviscid theory. Solutions that are limits of the viscous system solutions (analogous to the Orr–Sommerfeld equation in incompressible fluid) as viscosity vanishes are constructed such that the integration path is located in the complex z plane and passes below the critical point (Lees & Lin 1946; Lin 1966). In particular, if $\mathrm{Im}\, c > 0$ (growing disturbances), then integration can be accomplished along the real z axis. If $\mathrm{Im}\, c \leqslant 0$ (neutral and damped disturbances), integration must be accomplished in the complex z plane below the singularity.

A singularity at the critical point yields the fact that, for $c \in \mathbb{R}$, function $v(z)$ is complex and has a discontinuity at the critical point. If we choose c_1 and c_2 such that $v \in \mathbb{R}$ for $z > z_c$, then v discontinuously acquires an imaginary part for $z < z_c$. Physically, this means that when passing through the critical point, the phase of the disturbance is changed discontinuously. This discontinuity is absent in potential flow and can yield the stabilization or destabilization of disturbances by the boundary layer.

Substituting (3.2) into boundary conditions (2.5), finding c_1 and c_2, and calculating (3.3) yields the pressure disturbance on the plate surface:

$$p(0) = -\mu \left(\left(\frac{(M_\infty k - \omega)^2}{\sqrt{k^2 - (M_\infty k - \omega)^2}} \right)^{-1} + \left(\int_0^\delta \frac{T_0(\zeta)\,\mathrm{d}\zeta}{(u_0(\zeta) - c)^2} - \delta \right) \right)^{-1}. \tag{3.4}$$

The first term in parentheses represents the contribution of the uniform flow outside the boundary layer, whereas the second term represents the contribution of the boundary layer.

It is convenient to extract boundary layer thickness δ from the integral. Substituting $\zeta = \delta \eta$, we obtain the following:

$$\int_0^\delta \frac{T_0(\zeta)\,\mathrm{d}\zeta}{(u_0(\zeta) - c)^2} = \delta \int_0^1 \frac{T_0(\eta)\,\mathrm{d}\eta}{(u_0(\eta) - c)^2}. \tag{3.5}$$

Hereafter, we will consider functions $u_0(\eta)$ and $T_0(\eta)$ as describing the boundary layer profile, where η is the local boundary layer vertical coordinate, $0 \leqslant \eta \leqslant 1$.

Finally, the substitution of plate deflection $w(x, t) = \mathrm{e}^{\mathrm{i}(kx - \omega t)}$ and pressure disturbance $p = p(0)\mathrm{e}^{\mathrm{i}(kx - \omega t)}$ into the plate equation (2.1) yields the dispersion relation

$$\mathscr{D}(k, \omega) = (Dk^4 + M_w^2 k^2 - \omega^2)$$

$$- \mu \left(\left(\frac{(M_\infty k - \omega)^2}{\sqrt{k^2 - (M_\infty k - \omega)^2}} \right)^{-1} + \delta \left(\int_0^1 \frac{T_0(\eta)\,\mathrm{d}\eta}{(u_0(\eta) - c)^2} - 1 \right) \right)^{-1} = 0. \tag{3.6}$$

Note that its structure reflects the contribution of each of three media: the plate, the boundary layer, and the uniform flow outside the boundary layer. In particular, the expression in the first parentheses represents the plate: its three terms reflect the bending stiffness, tension, and inertia of the plate. The expression in the second parentheses represents the flow, whose influence is proportional to μ: the first term in parentheses is the contribution of the uniform flow, whereas the second term represents the boundary layer.

As $\delta \to 0$, the dispersion relation (3.6) coincides with the dispersion relation for a plate in uniform flow (Kornecki 1979; Vedeneev 2005):

$$(Dk^4 + M_w^2 k^2 - \omega^2) - \mu \frac{(M_\infty k - \omega)^2}{\sqrt{k^2 - (M_\infty k - \omega)^2}} = 0. \tag{3.7}$$

4. Instability of 'short' travelling waves in an infinite plate

In this section, we consider wavelengths that are not too long, so that solutions $\omega(k)$ of the dispersion relation for the plate in the flow are close to those for the plate in vacuum. In particular, we assume that $|k| \gg \mu^{1/3}$. The influence of the flow on such waves is small and can be taken into account in the first approximation in μ. On the other hand, we still restrict ourselves to the wavelengths that are much longer than the boundary layer thickness so that neglecting the term of the order of k^2 in (2.2) is correct. Thus, the wavelengths considered in this section are bounded both above and below, $\mu^{1/3} \ll |k| \ll 1/\delta$; this is why we have used quotation marks in the title of this section.

Under this assumption, the Taylor expansion in μ yields the following:

$$\omega(k, \mu) = \omega(k, 0) + \mu \left. \frac{\partial \omega}{\partial \mu} \right|_{\mu=0} + o(\mu) = \omega(k, 0) - \mu \left. \frac{\partial \mathscr{D}}{\partial \mu} \middle/ \frac{\partial \mathscr{D}}{\partial \omega} \right|_{\mu=0} + o(\mu). \tag{4.1}$$

Neglecting infinitesimal terms, we obtain

$$\omega(k, \mu) = \omega(k, 0) - \frac{\mu}{2\omega(k, 0)}$$

$$\times \left(\left(\frac{(M_\infty k - \omega)^2}{\sqrt{k^2 - (M_\infty k - \omega)^2}} \right)^{-1} + \delta \left(\int_0^1 \frac{T_0(\eta) \, d\eta}{(u_0(\eta) - c)^2} - 1 \right) \right)^{-1}, \tag{4.2}$$

where the expression in parentheses is calculated at $\mu = 0$.

It is seen that the frequency $\omega(k, \mu)$ of the plate in the flow can be represented as the frequency of the plate in vacuum $\omega(k, 0)$, slightly (to $O(\mu)$) modified by the flow. As the frequency in vacuum $\omega(k, 0)$ is always real, the stability of the plate in the flow is governed by this small term caused by the flow. The flow influence on the frequency, as well as on the dispersion relation, is clearly split into two different mechanisms expressed by two terms in parentheses: uniform flow (the first term) and the boundary layer (the second term).

In order to investigate the influence of the boundary layer on the growth of travelling waves, let us first consider waves in uniform flow, $\delta = 0$ (Vedeneev 2005). In this case, the behaviour of the wave is governed by the square root on the right-hand side of (4.2). The choice of an appropriate branch is not obvious and must be conducted by considering radiation condition (2.4) for rapidly growing waves. In other words, the square root branch must be an analytical continuation of the branch defined as follows:

$$\text{Re} \sqrt{k^2 - (M_\infty k - \omega)^2} > 0, \quad \text{Im} \, \omega \to +\infty, \tag{4.3}$$

from the region of very large $\text{Im} \, \omega$ to the values of interest. We will be primarily interested in unstable solutions, that is, $\text{Im} \, \omega > 0$; therefore, the path for continuation in the ω plane can be chosen so that it lies in the upper half-plane, and this continuation is single-valued (note that both branch points of the square root are

real for $k \in \mathbb{R}$). The accurate treatment of the continuation (Vedeneev 2005) yields four cases. If the wave propagates upstream (i.e. $c < 0$), it is always damped. If the wave propagates downstream, it is amplified if $0 < c < M_\infty - 1$, neutral if $M_\infty - 1 < c < M_\infty + 1$, and damped if $c > M_\infty + 1$. Physically, these inequalities express a relationship between the phase speed c of the wave running in the plate and the speed of acoustic waves $M_\infty \pm 1$ in the gas flow.

Thus, three types of wave behaviour are possible.

(i) In the uniform flow, the wave is growing and supersonic relative to the flow: $0 < c < M_\infty - 1$.

(ii) In the uniform flow, the wave is neutral and subsonic relative to the flow: $M_\infty - 1 < c < M_\infty + 1$.

(iii) In the uniform flow, the wave is damped and supersonic relative to the flow: $c > M_\infty + 1$ or $c < 0$.

Let us treat them in turn in order to investigate the influence of the boundary layer term in (4.2).

4.1. *Influence of the boundary layer on the growing wave*

First, we will investigate waves of type (i). To make the analysis clearer, let

$$A = \frac{\sqrt{k^2 - (M_\infty k - \omega)^2}}{(M_\infty k - \omega)^2} = \frac{\sqrt{1 - (M_\infty - c)^2}}{k(M_\infty - c)^2}, \quad B = \delta \left(\int_0^1 \frac{T_0(\eta)\,\mathrm{d}\eta}{(u_0(\eta) - c)^2} - 1 \right), \quad (4.4)$$

and rewrite (4.2):

$$\operatorname{Im}\omega(k, \mu) = -\frac{\mu}{2\omega(k, 0)}\operatorname{Im}(A + B)^{-1}. \quad (4.5)$$

Since the wave is growing at $\delta = 0$, we obtain $\operatorname{Im} A = a > 0$, $\operatorname{Re} A = 0$. Let us determine which regions of the B plane correspond to a decrease or increase of $\operatorname{Im}(A + B)^{-1}$ in comparison with $\operatorname{Im} A^{-1}$ (i.e. stabilization or destabilization of the wave by the boundary layer).

It is easy to prove that the level lines of $\operatorname{Im}(A + B)^{-1}$ on the complex B plane are circles with centres on the imaginary axis that pass through the point $B = -\mathrm{i}a$. If the second intersection of the circle and imaginary axis lies above this point, then $\operatorname{Im}(A + B)^{-1} < 0$; otherwise, $\operatorname{Im}(A + B)^{-1} > 0$. Level line $\operatorname{Im}(A + B)^{-1} = \operatorname{Im} A^{-1}$ is a circle that passes through the point $B = 0$. Level line $\operatorname{Im}(A + B)^{-1} = 0$ (neutral disturbances) is a horizontal line passing through the point $B = -\mathrm{i}a$ (figure 3).

Fix the phase speed c and consider $\operatorname{Im}(A + B)^{-1}$ as a function of the boundary layer thickness δ, assuming that profiles $u_0(\eta)$ and $T_0(\eta)$ are specified. A does not depend on δ, while B is a linear function of δ. Then values of B on the complex plane that correspond to different values of δ lie on a ray that begins at $B = 0$.

Two cases are possible. If $\operatorname{Im} B \geqslant 0$, then the ray is directed upward or horizontally. In this case, for any δ, the wave is growing; its growth rate is less than at $\delta = 0$ and tends to zero as $\delta \to \infty$.

In the other case, $\operatorname{Im} B < 0$, the ray is directed downward. For $0 < \delta < \delta_1$, the growth rate is positive and larger than at $\delta = 0$, where δ_1 is the value where the ray crosses the circle $\operatorname{Im}(A + B)^{-1} = \operatorname{Im} A^{-1}$ (figure 3). For $\delta_1 < \delta < \delta_2$, the growth rate is still positive, but less so than at $\delta = 0$, where δ_2 is the value at which the ray crosses the line $\operatorname{Im}(A + B)^{-1} = 0$. Finally, for $\delta > \delta_2$, the wave is damped.

The value of $\operatorname{Im} B$ is calculated explicitly as follows. The integrand in the definition of B has a singularity at the critical point $\eta = \eta_c$, which must be passed below,
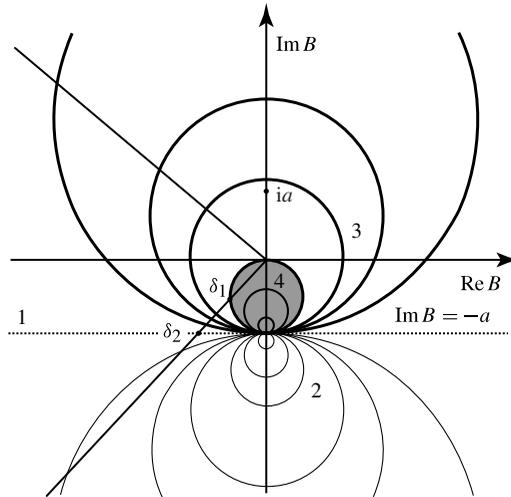
FIGURE 3. Level lines $\mathrm{Im}(A + B)^{-1}$: 1, $\mathrm{Im}(A + B)^{-1} = 0$; 2, set of lines below 1, $\mathrm{Im}(A + B)^{-1} > 0$; 3, set of lines above 1, $\mathrm{Im}\,A^{-1} < \mathrm{Im}(A + B)^{-1} < 0$; 4 (shaded), region $\mathrm{Im}(A + B)^{-1} < \mathrm{Im}\,A^{-1} < 0$.

according to Lin's rule. Let us expand boundary layer profiles in the Taylor series near $\eta = \eta_c$:

$$T_0(\xi) = T_{00} + T_{01}\xi + \cdots, \quad u_0(\xi) = c + u_{01}\xi + u_{02}\xi^2/2 + \cdots, \quad \xi = \eta - \eta_c, \quad (4.6)$$

where T_{0n} and u_{0n} are nth derivatives in the critical point. Then we have the following:

$$\frac{T_0(\xi)}{(u_0(\xi) - c)^2} = \frac{T_{00} + T_{01}\xi + \cdots}{(u_{01}\xi + u_{02}\xi^2/2 + \cdots)^2}$$

$$= \frac{T_{00}}{u_{01}^2}\frac{1}{\xi^2} + \frac{1}{u_{01}^2}\left(T_{01} - T_{00}\frac{u_{02}}{u_{01}}\right)\frac{1}{\xi} + \text{reg. terms.} \quad (4.7)$$

As the $1/\xi$ term is the only source of the non-zero imaginary part of B, we obtain

$$\mathrm{Im}\,B = \frac{\pi\delta}{u_{01}^2}\left(T_{01} - T_{00}\frac{u_{02}}{u_{01}}\right) = -\pi\delta\frac{T_0^2}{u_0'^3}\left(\frac{u_0'}{T_0}\right)', \quad (4.8)$$

where the prime denotes the derivative with respect to z at the critical point. Thus, $\mathrm{Im}\,B$ is a function of the boundary layer thickness and the local behaviour of the velocity and temperature profiles in a neighbourhood of the critical point. In contrast, the value of $\mathrm{Re}\,B$ depends on all regular terms in the expansion (4.7), i.e. on the profiles in the full segment $\eta \in [0; 1]$.

Let us now reformulate the results obtained in terms of the boundary layer profile. If the profile is generalized convex, i.e. $(u_0'/T_0)' < 0$ everywhere, then for any phase speed $\mathrm{Im}\,B > 0$. This means that the boundary layer has a stabilizing effect: although the growth rate in the flow with the boundary layer stays positive, it is less than in the uniform flow.

If the profile has a generalized inflection point, then there exists a range of phase speeds c such that the effect of the boundary layer is destabilizing (i.e. the growth rate of the wave in the flow with the boundary layer is higher than in the uniform flow)
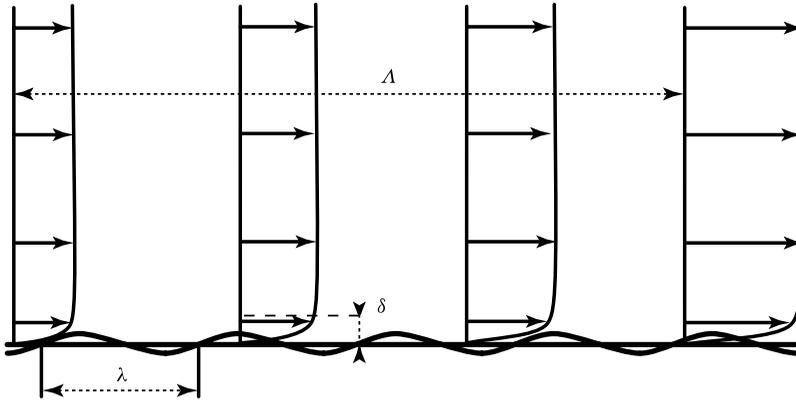
FIGURE 4. Length scale of accelerating outer flow Λ, boundary layer thickness δ, and the wavelength λ in the case of $\delta \ll \lambda \ll \Lambda$.

for $\delta < \delta_1$, since $\text{Im}\,B < 0$. The closer $|\text{Re}\,B|$ is to zero (i.e. the closer the direction of the ray to the vertical), the higher the growth rate due to the boundary layer. In the limit case $\text{Re}\,B = 0$, $\text{Im}\,B \to -a$ the value of $\text{Im}(A + B)^{-1}$ (and hence the growth rate $\text{Im}\,\omega$) tends to infinity as $\delta \to \delta_1$.

The possibility of very high growth rates caused by the boundary layer in real flows will be considered below in §§ 4.2 and 4.3. But the limit case of $c \to 0$ can be immediately excluded, as the behaviour of $\text{Re}\,B$ can be explicitly found. After the integration of (4.7), the leading term of $\text{Re}\,B$ is as follows:

$$\int_{-\eta_c}^{1-\eta_c} \frac{T_{00}}{u_{01}^2} \frac{1}{\xi^2} \mathrm{d}\xi = -\frac{T_{00}}{u_{01}^2} \frac{1}{\xi}\bigg|_{-\eta_c}^{1-\eta_c} = -\frac{T_{00}(\eta_c)}{u_{01}^2(\eta_c)} \left(\frac{1}{1 - \eta_c} + \frac{1}{\eta_c} \right). \tag{4.9}$$

Thus, as $c \to 0$ (consequently, $\eta_c \to 0$), $\text{Re}\,B \to -\infty$, i.e. the ray direction tends to horizontal. This means that, first, $\delta_1 \to 0$ and, second, the increase of the growth rate caused by the boundary layer for $0 < \delta < \delta_1$ is negligible. We conclude that destabilization of the wave growing in uniform flow by the boundary layer can occur only for intermediate phase speeds, $0 < c < M_\infty - 1$.

4.2. *Example: profiles of accelerating and decelerating flows*

Consider self-similar boundary layer profiles (Schlichting 1960) that are governed by parameter β. If $\beta > 0$, then the free-stream flow is accelerating; if $\beta < 0$, then it is decelerating; if $\beta = 0$, then the flow velocity is constant. These profiles are analogous to those boundary layer profiles that appear in incompressible fluid in the case of degree function flow $u_\infty(x) = Cx^m$, $\beta = 2m/(m + 1)$. Note that the problem of an infinite-length plate is treated here for the purpose of using its solutions to construct eigenmodes of a finite-length plate, which will be considered in § 6. We will assume that the plate length is much less than the characteristic distance Λ, over which the flow outside the boundary layer essentially changes; hence, the flow can be considered as locally uniform. This assumption can be also applied to the infinite-length plate if we are interested only in the local behaviour of the piece of the wave, whose length λ is much smaller than the length scale Λ of the flow outside the boundary layer (figure 4). Although there exist beautiful theories for constructing global modes of the infinite plate in a slowly varying flow in both linear (Huerre & Monkewitz 1990;

Hunt & Crighton 1991; Le Dizès *et al.* 1996) and nonlinear (Pier, Huerre & Chomaz 2001; Chomaz 2005) formulations, in this section, we only study the effect of the local flow profile, and global modes of the infinite plate are not considered in this paper. In other words, when we refer to 'accelerating' and 'decelerating' flow hereafter, we mean the corresponding boundary layer profile, still considering the free-stream flow to be uniform.

In this section, we consider an example of the Prandtl number $Pr = 1$ and the heat-insulated plate so that the boundary layer profiles are expressed via the solution $f(\xi)$ of the following equation (Schlichting 1960):

$$f''' + ff'' = \beta(f'^2 - 1), \quad f(0) = f'(0) = 0, \quad f'(+\infty) = 1. \tag{4.10}$$

Velocity is then given as a function of a similarity variable ξ: $u_0(\xi) = f'(\xi)$. The physical z coordinate is calculated for each ξ as follows:

$$z = C \int_0^\xi T_0(u_0(\xi)) \, d\xi. \tag{4.11}$$

Temperature profile $T_0(u_0)$ is given using the same expression as in adiabatic flow:

$$T_0(u_0) = 1 + \frac{\gamma - 1}{2}(M_\infty^2 - u_0^2). \tag{4.12}$$

Let us consider several profiles as examples. They are denoted as 1–5 in figure 5(*a*) and correspond to $\beta = 2$, 0.5, 0, -0.14 and -0.199, respectively. Note that profile 5 is a limit case of the attached boundary layer, because $du_0(0)/dz < 0$ for $\beta < -0.199$, and the boundary layer separates from the plate. Calculations have been conducted for parameters that correspond to a steel plate at 3 km above sea level:

$$D = 23.9, \quad M_w = 0, \quad \mu = 0.00012, \quad \gamma = 1.4, \tag{4.13}$$

and Mach number $M_\infty = 1.6$. The generalized curvature $(u_0'/T_0)'$ is plotted for these profiles in figure 5(*b*), while values of $\mathrm{Re}\,B$ and $\mathrm{Im}\,B$ are shown in figures 5(*c*) and 5(*d*). It is seen in figure 5(*d*) that for profiles 1 and 2, $\mathrm{Im}\,B > 0$, and the growth rate decreases when δ increases. This is also seen in figure 6, where $\mathrm{Im}\,\omega$ is plotted versus the boundary layer thickness for a particular wavenumber $k = 0.06$. In the case of profiles 3–5, $\mathrm{Im}\,B < 0$ for waves travelling with supersonic speed relative to the outer flow (i.e. for $c < M - 1$), which means that the wave is amplified by the boundary layer at $\delta < \delta_1$ (figure 6). As proved in § 4.1, the smallness of $|\mathrm{Re}\,B|$ is a condition of the significant destabilizing effect of the boundary layer. It is seen in figure 5(*c*) that amongst the profiles considered, $|\mathrm{Re}\,B|$ is the smallest for profile 5 on a whole interval $c < M_\infty - 1$. According to this, $\mathrm{Im}\,\omega$ is significantly increased for this profile by the boundary layer (figure 6).

4.3. *Relation between the effect of the boundary layer on the stability of an elastic plate and the stability of the boundary layer over a rigid wall*

Let us now investigate the influence of the boundary layer on the plate stability in relation to the stability of the boundary layer over a rigid wall. Boundary conditions for the Rayleigh equation (2.2) in the latter case are as follows:

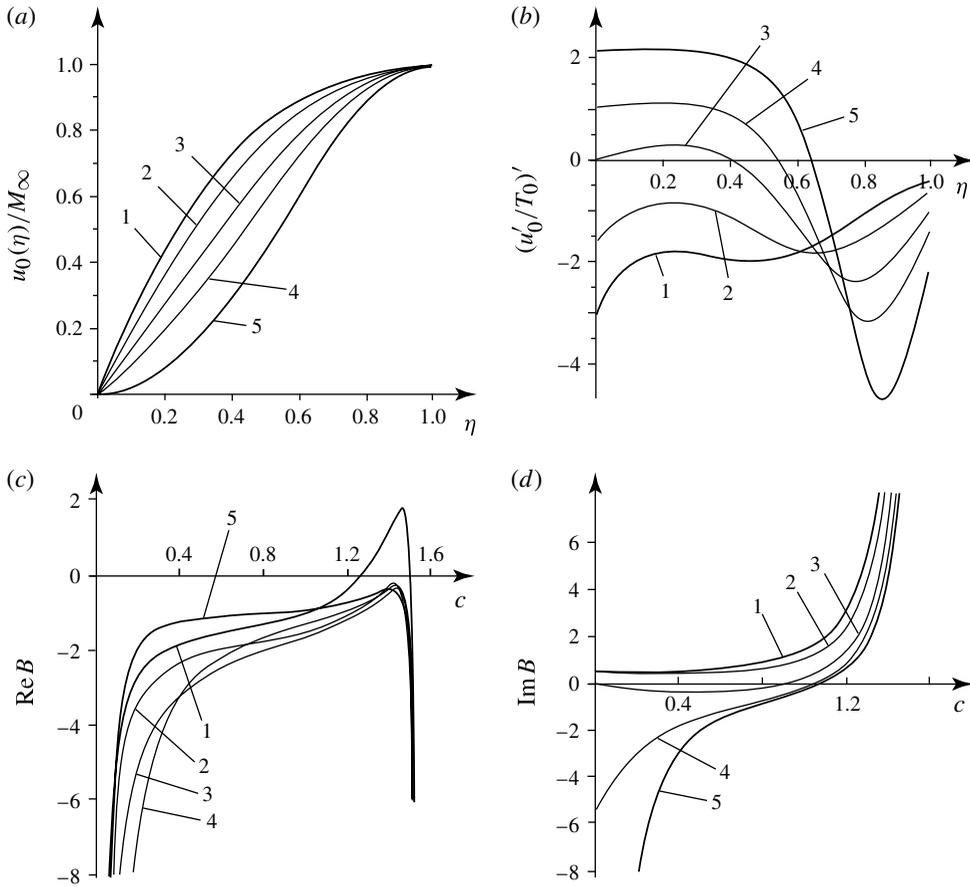$$v = 0, \quad z = 0, \quad \frac{1}{v}\frac{dv}{dz} = \gamma, \quad z = 1. \tag{4.14}$$

FIGURE 5. Velocity profiles for accelerating and decelerating flows over a heat-insulated plate for parameters (4.13), $M_\infty = 1.6$, $Pr = 1$: (*a*) velocity profiles, (*b*) generalized curvature, (*c*) Re B, (*d*) Im B. Curves 1–5 correspond to $\beta = 2.0, 0.5, 0.0, -0.14, -0.199$, respectively.

Taking the general solution (3.2) and satisfying boundary conditions (4.14), we obtain the eigenvalue problem

$$\left(\frac{(M_\infty k - \omega)^2}{\sqrt{k^2 - (M_\infty k - \omega)^2}}\right)^{-1} + \delta\left(\int_0^1 \frac{T_0(\eta)\,\mathrm{d}\eta}{(u_0(\eta) - c)^2} - 1\right) = 0, \qquad (4.15)$$

which is rewritten in the following form:

$$A + B = 0. \qquad (4.16)$$

Solutions of this equation give a spectrum of eigenvalues c for a given wavenumber $|k| \ll 1/\delta$; if Im $c > 0$ for at least one of them, then the boundary layer is unstable.

In the inviscid stability theory of compressible shear flows, two different stability criteria are obtained for subsonic ($c > M_\infty - 1$) and supersonic ($c < M_\infty - 1$) waves (Lees & Lin 1946). The criterion for subsonic waves is analogous to the incompressible inflection-point criterion, and the regular inflection point, where $u_0'' = 0$, is replaced by the generalized inflection point, where $(u_0'/T_0)' = 0$. The criterion for supersonic waves is completely different and has no relation to the inflection point.
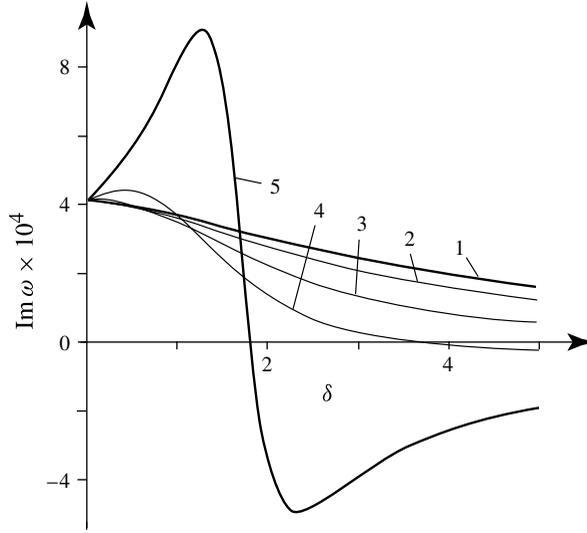
FIGURE 6. Function $\operatorname{Im}\omega(\delta)$ for profiles 1–5 in figure 5 for parameters (4.13), $M_\infty = 1.6$, $k = 0.06$.

Let us now review these criteria through the long-wave approximation (4.16) of the eigenvalue problem and relate them to the effect of the boundary layer on the stability of the elastic plate. If the boundary layer is unstable, then there exists a neutral disturbance that lies on a boundary of the region of unstable wavenumbers. If this disturbance is supersonic (i.e. $c \in [0; M_\infty - 1]$), then $\operatorname{Re}A = 0$, $\operatorname{Im}A > 0$. It follows from (4.16) that $\operatorname{Re}B = 0$, $\operatorname{Im}B < 0$; hence, the ray in figure 3 is directed straight down. Thus, for the instability of long supersonic waves over the rigid wall, it is necessary that the ray in figure 3 is directed straight down at a certain $c \in [0; M_\infty - 1]$, whereas for the significant increase of the growth rate of the plate waves by the boundary layer, it is sufficient that the ray direction is just close to being straight down.

If the neutral disturbance is subsonic (i.e. $M_\infty - 1 < c < M_\infty + 1$), then $\operatorname{Im}A = 0$, and the necessary condition for instability follows from (4.16): $\operatorname{Im}B = 0$, that is, there exists a point in the subsonic part of the boundary layer where $(u'_0/T_0)' = 0$. We call this point the generalized inflection point of the profile. This condition is actually necessary and sufficient without the assumption of small k (Lees & Lin 1946; Lin 1966). Note that if a subsonic neutral disturbance exists (i.e. there exists a generalized inflection point), then only subsonic waves can be growing (Lees & Reshotko 1962).

Taking these general criteria into account, let us analyse the stability of the profiles considered in §4.2. They all are stable with respect to long supersonic waves. Indeed, it is seen in figure 5 that $\operatorname{Re}B \neq 0$ for any real $c < M_\infty - 1$, although $\operatorname{Re}B$ can be sufficiently small for $\beta = -0.199$, which gives a significant increase of $\operatorname{Im}\omega$ for $\delta < \delta_1$ (figure 6). However, at $\beta = 0, -0.14, -0.199$, the boundary layer is unstable with respect to subsonic disturbances because there exists a point in the subsonic part of the layer where $\operatorname{Im}B = 0$ (figure 5*d*). We conclude that profiles that affect the plate stability in a destabilizing manner cannot actually develop over a plate due to their own instability. The question that arises is as follows: Does a profile that, on one hand, is stable over a rigid wall (i.e. can actually develop) and that, on the other hand, destabilizes the plate exist?

The answer to this question turns out to be positive. Indeed, if the boundary layer profile has a generalized inflection point that lies in the supersonic part of the layer, such a layer can be stable (in inviscid approximation). It can also yield an arbitrarily large growth rate of the plate waves if $\mathrm{Im}\, B < 0$ and $\mathrm{Re}\, B$ is negative and close to zero for $c \in [0; M_\infty - 1]$. For the stability of the layer over the rigid wall, it should be $\mathrm{Re}\, B \neq 0$ for $c \in [0; M_\infty - 1]$ (supersonic disturbances) and $\mathrm{Im}\, B \neq 0$ for $c \in [M_\infty - 1; M_\infty]$ (subsonic disturbances).

As an example of such profiles, consider temperature profile (4.12) and the family of velocity profiles $u_0(\eta)$ parametrized by a parameter $s \in [0; 1]$, which are defined through a natural cubic spline passing through the following five points:

$$\left. \begin{aligned} u_0(0) = 0, \quad u_0(0.105 - 0.045s) = 0.12 M_\infty, \\ u_0(0.155 - 0.045s) = 0.21 M_\infty, \quad u_0(0.6) = 0.88 M_\infty, \quad u_0(1) = M_\infty. \end{aligned} \right\} \quad (4.17)$$

Here, the first, fourth, and fifth points are fixed, whereas the second and third points shift with the change in s. Plots of $u_0(\eta)$ for several values of s are shown in figure 7(*a*). It is seen that the increase of s makes the profile more convex and eliminates the generalized inflection point. Note that when defining a profile using a cubic spline, which is a function with continuous first and second derivatives, we assume that the spline can be approximated (including the first and second derivatives) arbitrarily well by an analytic function.

Plots of $\mathrm{Re}\, B(c)$ and $\mathrm{Im}\, B(c)$ for these profiles are shown in figures 7(*c*) and 7(*d*) for $c \in [0; M_\infty - 1]$. All these profiles are stable with respect to subsonic disturbances as $(u_0'/T_0)' \neq 0$ for $c > M_\infty - 1$ (figure 7*b*), and the generalized inflection point, if it exists, lies in the part of the layer which is supersonic relative to the outer flow. At $s = 0$, a graph of $\mathrm{Re}\, B(c)$ touches the horizontal axis, which means that there exists a neutral supersonic wave; for $s > 0$, supersonic waves are damped as $\mathrm{Re}\, B \neq 0$ for $c < M_\infty - 1$. Thus, all these profiles are stable.

Now consider the influence of these boundary layers on the stability of the elastic plate. As $s \to 0$, the ray in figure 3 tends to be vertical at $c \approx 0.21$ (where the graph of $\mathrm{Re}\, B$ touches the horizontal axis in figure 7*c*), which yields an arbitrarily high growth rate as $\delta \to \delta_1$. Calculated $\mathrm{Im}\, \omega(\delta)$ are shown in figure 8 for parameters (4.13), $M_\infty = 1.3$. It is seen that max $\mathrm{Im}\, \omega$ is increased more than twice in comparison with the uniform flow at $s = 0.2$, and more than four times at $s = 0.1$, max $\mathrm{Im}\, \omega \to +\infty$ as $s \to 0$.

Note that an arbitrarily high growth rate contradicts the assumptions that were used when deriving expansion (4.2), since it will no longer be linear in μ. In fact, we can only conclude that $\mathrm{Im}\, \omega \gtrsim \mu$. This situation is analogous to that considered by Vedeneev (2006): the growth rate is also unbounded in uniform flow as $c \to M_\infty - 1$ because of the first term in parentheses in (4.2); in that case, a nonlinear expansion in μ yields $\mathrm{Im}\, \omega \sim \mu^{2/3}$.

4.4. *Influence of the boundary layer on neutral and damped waves*

We have investigated the influence of the boundary layer on waves that are growing in potential flow, that is, $0 < c < M_\infty - 1$. Now suppose that the wave is damped in potential flow, that is, $M_\infty + 1 < c$ or $c < 0$. Then A is purely imaginary, and $\mathrm{Im}\, A < 0$. There is no critical point in the flow; therefore, $\mathrm{Im}\, B = 0$. Then $0 < \mathrm{Im}\, (A + B)^{-1} < \mathrm{Im}\, A^{-1}$, which means that the boundary layer decreases the wave's damping rate but cannot result in its growth. Damped waves stay damped.
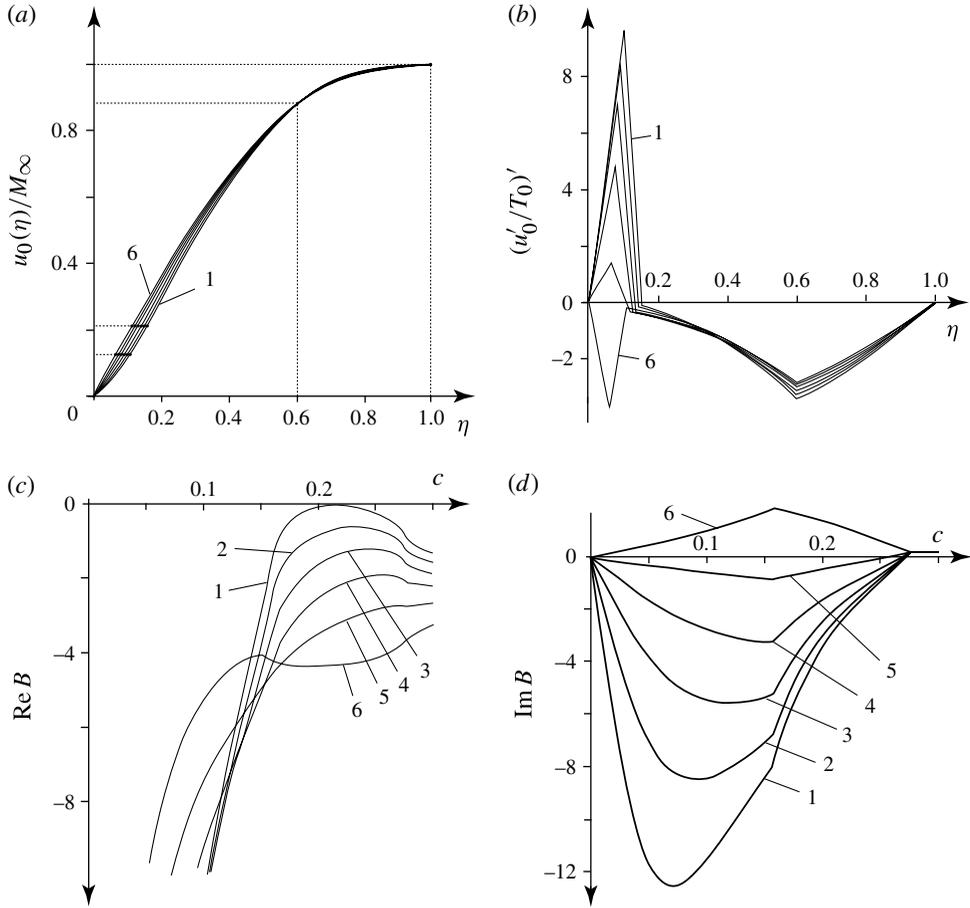
FIGURE 7. Boundary layer profiles (4.17) for a heat-insulated plate for parameters (4.13), $M_\infty = 1.3$, $Pr = 1$: (*a*) velocity profiles, (*b*) generalized curvature, (*c*) Re B, (*d*) Im B. Curves 1–6 correspond to $s = 0$, 0.2, 0.4, 0,6, 0.8, 1, respectively.

Next, suppose that the wave is neutral in uniform flow, that is, $M_\infty - 1 < c < M_\infty + 1$, and Im $A = 0$. If $M_\infty \leqslant c \leqslant M_\infty + 1$, then there is no critical point in the flow; therefore, Im $B = 0$. The wave stays neutral in the boundary layer.

If the wave in uniform flow is neutral and $M_\infty - 1 < c < M_\infty$, then there is a critical point, and Im $B \neq 0$. Consider two types of the boundary layer profile. In the case of the flow with a generalized convex profile, $(u_0'/T_0)' < 0$, sign Im $B = -\text{sign}((u_0'/T_0)') > 0$. Consequently, Im $(A + B)^{-1} < 0$ and Im $\omega > 0$, which means that the wave is destabilized by the boundary layer. Note that the boundary layer itself (i.e. over a rigid wall) is stable. This conclusion is similar to that obtained by Miles (2001), who showed that for the Blasius boundary layer in incompressible fluid, elasticity of the plate yields destabilization of the layer as Re $\rightarrow \infty$.

Finally, suppose that the boundary layer profile has a generalized inflection point z_{infl} in the subsonic part of the layer so that $(u_0'/T_0)' > 0$ for $z < z_{infl}$ and $(u_0'/T_0)' < 0$ otherwise (this is typical for boundary layers over a flat heat-insulated plate; we restrict ourselves to this class of boundary layers). Then waves that have critical points at $z > z_{infl}$, that is, $M_\infty - 1 < u_0(z_{infl}) < c < M_\infty$, are destabilized by the boundary
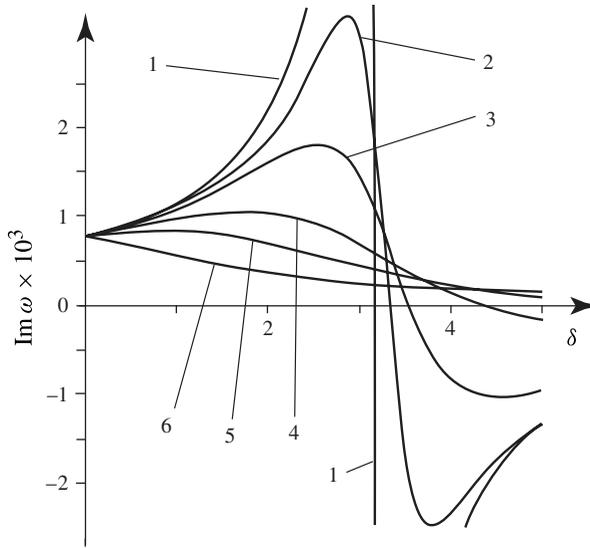
FIGURE 8. Function $\mathrm{Im}\,\omega(\delta)$ for profiles (4.17) at parameters (4.13), $M_\infty = 1.3$, $k = 0.043$ ($c \approx 0.21$); curves 1–6 correspond to $s = 0, 0.1, 0.2, 0.4, 0.6, 1$, respectively.

layer because $\mathrm{sign}\,\mathrm{Im}\,B = -\mathrm{sign}((u_0'/T_0)') > 0$ and hence $\mathrm{Im}\,(A+B)^{-1} < 0$. In contrast, waves with phase speeds such that $M_\infty - 1 < c < u_0(z_{infl})$ become damped.

5. Instability of long travelling waves in an infinite plate: absolute and convective instability

In the previous sections we have treated waves that are not too long, i.e. $k \gg \mu^{1/3}$. Now consider wavenumbers $k \sim \mu^{1/3}$, which we will refer to as long waves. Vedeneev (2005) showed that the instability of long plate waves in uniform flow is absolute for small plate tension and convective for large tension. In this section, we will prove that when instability in uniform flow is absolute, it stays absolute in the presence of the boundary layer. If instability in uniform flow is convective, it becomes absolute. Thus, in the presence of the boundary layer, instability is always absolute. That is why instead of treating ordinary instability of long waves first, we will directly investigate absolute instability.

5.1. *Absolute instability criterion*

Consider the perturbation that at $t = 0$ is localized in a neighbourhood of a point $x = x_0$. The question answered by an absolute instability analysis is as follows: If the system is unstable, will this localized perturbation grow at the point $x = x_0$ (in this case, instability is absolute), or will it travel along the x axis such that it damps at $x = x_0$ as $t \to \infty$ (in this case, instability is convective), as shown in figure 9?

An absolute instability analysis (Briggs 1964; Whitham 1974; Bers 1983; Huerre & Monkewitz 1985) is based on expressing an initial localized perturbation in the form of superpositioned travelling waves, whose frequency ω and wavenumber k are connected to each other by the dispersion relation (3.6). Its solution $\omega(k)$ is a multivalued function for which each branch $\omega_j(k)$ gives a single temporally developing wave. From a mathematical point of view, such a representation of the localized
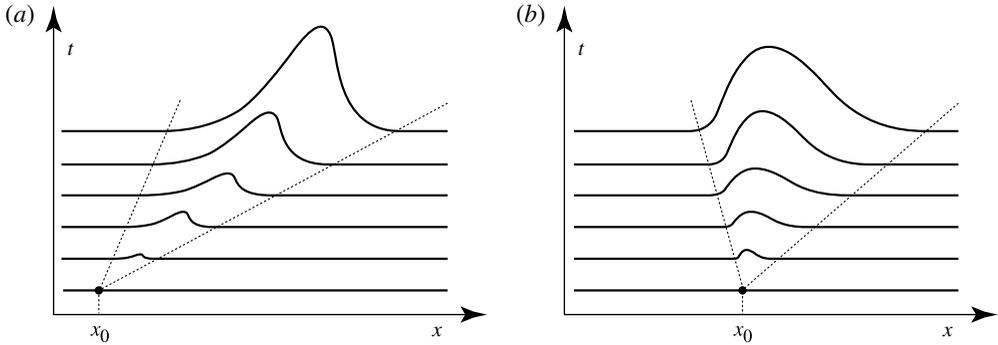
FIGURE 9. Evolution of localized disturbance: (*a*) convective and (*b*) absolute instability.

perturbation is given by the Fourier transform:

$$w(x, t) = \int_{-\infty}^{\infty} \sum_{j=1}^{n} W_j(k) e^{i(kx - \omega_j(k)t)} \, dk, \tag{5.1}$$

where integration is conducted along the real k axis. We are interested in the behaviour of $w(x_0, t)$ as $t \to \infty$. The calculation of the integral (5.1) is performed by deforming the integration contour in the k plane and employing the method of steepest descent. In particular, we deform the integration contour in the complex k plane such that it passes through saddle points of the function $\omega_j(k)$ for each single-valued j branch. These saddle points satisfy the following equation:

$$\frac{d\omega_j(k)}{dk} = 0. \tag{5.2}$$

Then the asymptotic behaviour of $w(x_0, t)$ as $t \to \infty$ is as follows:

$$w(x_0, t) \sim A W(k_b) \sqrt{\frac{2\pi}{|\omega''(k_b)|}} \frac{e^{i(k_b x_0 - \omega_b t)}}{\sqrt{t}}, \tag{5.3}$$

where $|A| = 1$; (k_b, ω_b) is one of the saddle points of $\omega_j(k)$, which has the greatest $\mathrm{Im}\,\omega$ amongst the saddle points through which the contour passes. It is seen that the absolute instability criterion is then as follows: if there is a point k_b satisfying (5.2), through which the integration contour passes so that $\mathrm{Im}\,\omega_b > 0$, then the system is absolutely unstable. Otherwise, instability is convective.

The main difficulty in applying the absolute instability criterion is that not all saddle points (5.2) give asymptotic behaviour because the integration contour does not necessarily pass through all of them. In order to select branch points that govern absolute instability, one needs to investigate the topology of level lines of the multivalued function $\mathrm{Im}\,\omega(k)$. This yields a saddle point selection criterion based on the investigation of the integration contour.

We will use another selection criterion, which is equivalent to the one based on the analysis of the integration contour. In order to formulate this criterion, let us consider the inverse solution of the dispersion relation $k(\omega)$. It is a multivalued function for which each branch $k_l(\omega)$ represents a spatial wave. Let us split these branches into two groups. The first group, $l = 1, \ldots, s$, is such that $\mathrm{Im}\,k_l(\omega) \to +\infty$ as $\mathrm{Im}\,\omega \to +\infty$, whereas the second group, $l = s+1, \ldots, N$, is such that $\mathrm{Im}\,k_l(\omega) \to -\infty$

as $\text{Im}\,\omega \to +\infty$. Branches belonging to the first group correspond to spatial waves travelling downstream, while those belonging to the second group correspond to waves travelling upstream. Now describe the selection criterion. Let k_b be a saddle point of $\omega(k)$, i.e. the value satisfying (5.2) for some j. The frequency $\omega_b = \omega_j(k_b)$ is then a branch point of the inverse function $k(\omega)$, which means that two k branches merge: $k_p(\omega_b) = k_q(\omega_b)$. Then the selection criterion of saddle points that are responsible for absolute instability is as follows: merged branches must belong to different groups. It is easy to prove that the maximum of $\text{Im}\,\omega$ taken over selected branch points does not depend on which of the selection criteria is used: based either on the integration contour analysis or on an analysis of merged branches $k_l(\omega)$. Hence, both selection criteria yield an absolute instability criterion.

5.2. *Simplification of the dispersion relation*

In the uniform flow ($\delta = 0$), the branch point of $k(\omega)$ responsible for absolute instability satisfies inequality $|\omega| \ll |k|$, namely, $k \sim \mu^{1/3}$, $\omega \sim \mu^{2/3}$ (Vedeneev 2005). We will prove that the same orders of k and ω hold for $\delta \neq 0$ so that we may simplify the dispersion relation (3.6). First, in the first term in parentheses, we may neglect ω in comparison with $M_\infty k$, i.e. substitute

$$\frac{(M_\infty k - \omega)^2}{\sqrt{k^2 - (M_\infty k - \omega)^2}} \to -\mathrm{i}\frac{M_\infty^2}{\sqrt{M_\infty^2 - 1}}k. \tag{5.4}$$

The choice of the square root branch is justified by Vedeneev (2005).

Second, we may simplify the integral term. Note that in the branch point of our interest $c = \omega/k \sim \mu^{1/3}$. Due to the no-slip condition for unperturbed flow $u_0(0) = 0$, then the critical point η_c, where $u_0(\eta_c) = c$, can be approximated as follows: $\eta_c \approx c/u_0'(0) \sim \mu^{1/3}$. This point is a pole of the integrand that lies in a small neighbourhood of the left end of the integration interval $\eta = 0$. Hence, the main contribution to the integral is from this neighbourhood. Taking expansion (4.7) into account, it is seen that as $c \to 0$, the leading-order term in the integral is

$$\int_{-\eta_c}^{1-\eta_c} \frac{T_{00}}{u_{01}^2}\frac{1}{\xi^2}\mathrm{d}\xi = -\frac{T_{00}}{u_{01}^2}\frac{1}{\xi}\bigg|_{-\eta_c}^{1-\eta_c} = -\frac{T_{00}(\eta_c)}{u_{01}^2(\eta_c)}\left(\frac{1}{1-\eta_c} + \frac{1}{\eta_c}\right) \to -\frac{T_0(0)}{u_0'(0)}\frac{1}{c}. \tag{5.5}$$

Therefore, the dispersion relation (3.6) has the following asymptotic form as $\mu \to 0$:

$$\mathscr{D}(k, \omega) = (Dk^4 + M_w^2 k^2 - \omega^2) - \mu\left(\mathrm{i}\frac{\sqrt{M_\infty^2 - 1}}{M_\infty^2}\frac{1}{k} - \delta\frac{T_0(0)}{u_0'(0)}\frac{k}{\omega}\right)^{-1} = 0. \tag{5.6}$$

It is seen that for the orders of k and ω assumed above, both terms in parentheses of (5.6) are of the same order $\mu^{-1/3}$.

It is convenient to rewrite (5.6) in the following form:

$$\mathscr{D}(k, \omega) = (Dk^4 + M_w^2 k^2 - \omega^2) - \frac{\mu\omega k}{\mathrm{i}a\omega - \delta b k^2} = 0, \tag{5.7}$$

where

$$a = \frac{\sqrt{M_\infty^2 - 1}}{M_\infty^2} > 0, \quad b = \frac{T_0(0)}{u_0'(0)} > 0. \tag{5.8}$$

Saddle points of solutions of (5.7) $\omega(k)$ (i.e. branch points of $k(\omega)$) are given by (5.2), which yields the condition $\partial \mathscr{D} / \partial k = 0$:

$$4Dk^3 + 2M_w^2 k - \frac{\mu \omega \left(\mathrm{i}a\omega + \delta b k^2\right)}{\left(\mathrm{i}a\omega - \delta b k^2\right)^2} = 0. \tag{5.9}$$

In order to seek branch points, instead of (5.7), we will use the equivalent equation obtained by multiplying (5.7) by 4 and subtracting (5.9) multiplied by k:

$$2M_w^2 k^2 - 4\omega^2 + \frac{\mu \omega k \left(-3\mathrm{i}a\omega + 5\delta b k^2\right)}{\left(\mathrm{i}a\omega - \delta b k^2\right)^2} = 0. \tag{5.10}$$

Thus, the branch points of the multivalued function $k(\omega)$ are the roots of the system (5.9), (5.10). Generally speaking, not all the roots of this system satisfy the condition of $z = 0$ not lying in the WKB region (figure 2); that is, some of the roots need viscosity to be taken into account even for an arbitrarily large Reynolds number. We cannot exclude the situation when such branch points yield absolute instability, as in the study of Wiplier & Ehrenstein (2001), where absolute instability is generated by coincidence of the Tollmien–Schlichting wave caused by the boundary layer and a wave caused by the plate. However, due to the small growth rates of Tollmien–Schlichting waves in comparison with the growth rates of flutter, we assume that such an absolute instability is weak compared with flutter. That is why we restrict ourselves to a particular problem: the investigation of the boundary layer influence on a particular branch point that is responsible for flutter in uniform flow. It will be seen that at this point, $\mathrm{Im}\,c > 0$; hence, its investigation in inviscid approximation is correct.

To choose branch points responsible for instability, we will establish a connection between branch points and the topology of level lines of $\mathrm{Re}\,\omega(k)$ in the following manner. Take certain parameters of the problem and numerically plot level lines of $\mathrm{Re}\,\omega(k)$. Mark saddle points of $\omega(k)$ and select those that govern absolute instability. Next, when changing parameters, it is enough to watch only the location of the marked points (which can be done analytically) because the topology of the level lines is not changed if the parameters are not changed much. If bifurcation of the branch points occurs, then a connection to a new topology of the level lines must be established anew, though again for certain parameter values. To establish the connection, we will use the following parameters:

$$D = 23.9, \quad M_\infty = 1.5, \quad \mu = 0.00012. \tag{5.11}$$

Dimensionless bending stiffness and flow density are the same as in (4.13); however, we will include plate tension because it significantly changes the location of the branch points.

Let us discuss the splitting of the roots $k_l(\omega)$ of (5.7) into two groups (§ 5.1). At $\delta = 0$, there are four roots $k_l(\omega)$, two in each group: $\mathrm{Im}\,k_{1,2}(\omega) \to +\infty$, $\mathrm{Im}\,k_{3,4}(\omega) \to -\infty$ as $\mathrm{Im}\,\omega \to +\infty$. For large $|\omega|$, they are close to the roots of (5.7) at $\mu = 0$, i.e. to roots of the dispersion relation for the plate in vacuum. For $\delta \neq 0$, two more roots appear: one of them tends to $+\mathrm{i}\infty$, the other to $-\mathrm{i}\infty$ as $\mathrm{Im}\,\omega \to +\infty$. For large $|\omega|$, they are close to the roots of the denominator of the fraction in (5.7). We will use $k_{bl+}(\omega)$ to denote the first additional root and $k_{bl-}(\omega)$ for the second. Now each group consists of three roots: k_1, k_2, k_{bl+} and k_3, k_4, k_{bl-}.

We will investigate the location of the branch points in the half-plane $\mathrm{Re}\,\omega \geqslant 0$ because a frequency ω reflected from the imaginary axis corresponds to the solution of

$k(\omega)$ of (5.7) also being reflected from the imaginary axis. Physically, such reflected roots correspond to the same wave.

5.3. *A plate in uniform gas flow*

If $\delta = 0$, then the system (5.9), (5.10) is reduced to

$$4Dk^3 + 2M_w^2 k + \frac{i\mu}{a} = 0, \tag{5.12a}$$

$$2M_w^2 k^2 - 4\omega^2 + 3\frac{i\mu}{a}k = 0, \tag{5.12b}$$

which has been studied by Vedeneev (2005). Let us review the results of that investigation here.

When $M_w = 0$ (no plate tension), there are three branch points in k plane that correspond to $\mathrm{Re}\,\omega \geqslant 0$; the topology of level lines is shown in figure 10(a). The first point,

$$k^* = \left(\frac{\mu}{4Da}\right)^{1/3} e^{-i\pi/6}, \quad \omega^* = \frac{\sqrt{3}}{2}\left(\frac{\mu}{a}\right)^{2/3} \frac{1}{(4D)^{1/6}} e^{i\pi/6}, \tag{5.13}$$

is responsible for absolute instability, due to the coincidence of branches k_2 and k_4 from different groups at this point. At the second point,

$$k^{**} = \left(\frac{\mu}{4Da}\right)^{1/3} e^{-5i\pi/6}, \quad \omega^{**} = \frac{\sqrt{3}}{2}\left(\frac{\mu}{a}\right)^{2/3} \frac{1}{(4D)^{1/6}} e^{-i\pi/6}, \tag{5.14}$$

coincidence of the branch k_3 and the branch arising from the first point occurs. This point has no relation to instability as $\mathrm{Im}\,\omega^{**} < 0$. At the third point,

$$k^{***} = \left(\frac{\mu}{4Da}\right)^{1/3} i, \quad \omega^{***} = \pm\frac{\sqrt{3}}{2}\left(\frac{\mu}{a}\right)^{2/3} \frac{1}{(4D)^{1/6}} i, \tag{5.15}$$

branches k_1 and k_2 from the same group coincide; hence, this point also has no relation to instability.

While increasing M_w such that

$$M_w < M_w^{cr} = \sqrt{\frac{3}{2}}\left(\frac{\mu}{a}\right)^{1/3} D^{1/6}, \tag{5.16}$$

the frequencies ω^* and ω^{**} approach the real axis but stay in the same quadrants of the complex ω plane as at $M_w = 0$.

At $M_w = M_w^{cr}$, bifurcation of the branch points occurs (figure 10b). The first and the second points coincide at the real ω axis:

$$\omega^* = \omega^{**} = \frac{\sqrt{3}}{4}\left(\frac{\mu}{a}\right)^{2/3} \frac{1}{D^{1/6}} \tag{5.17}$$

and stay real for $M_w > M_w^{cr}$. In the k plane, the coincidence of the branch points occurs on the imaginary axis:

$$k^* = k^{**} = -\frac{i}{2}\left(\frac{\mu}{Da}\right)^{1/3}. \tag{5.18}$$

For $M_w > M_w^{cr}$, they stay pure imaginary. The topology of level lines (figure 10c) shows that for $M_w > M_w^{cr}$ amongst two branch points, the one responsible for
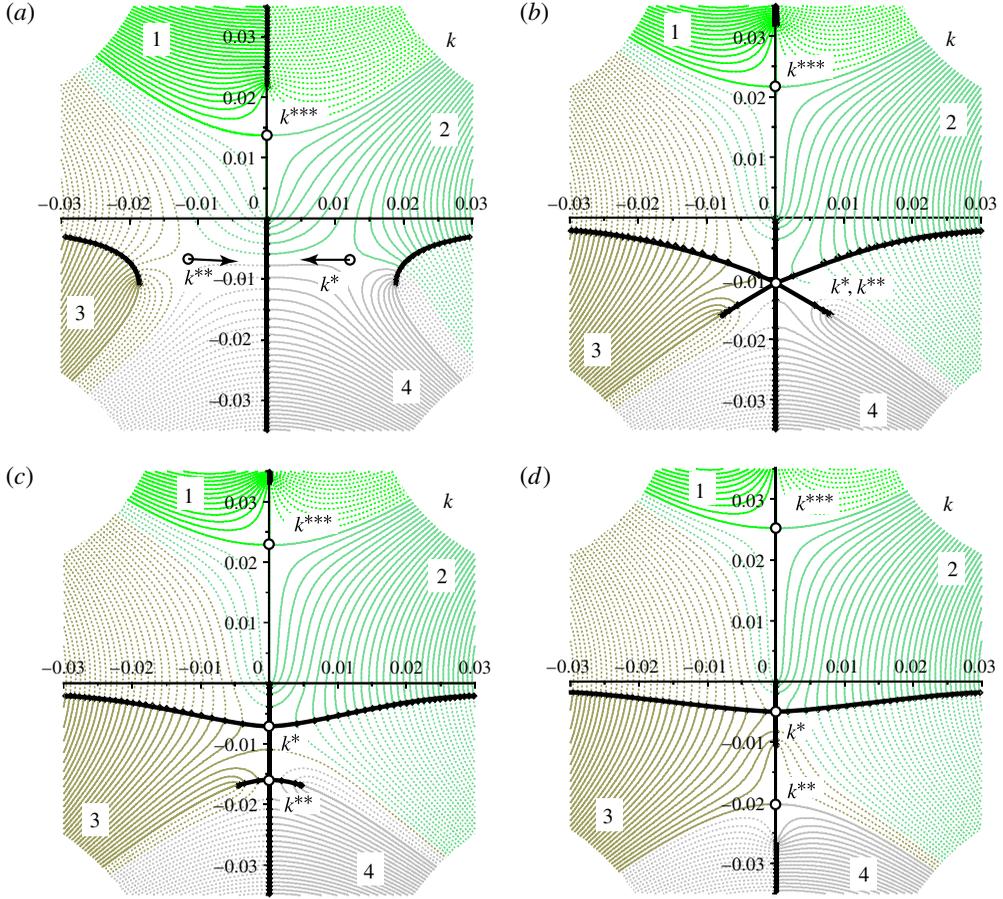
FIGURE 10. (Colour online) Level lines $\operatorname{Re}\omega(k) = \text{const.} \geqslant 0$ in the complex k plane for parameters (5.11): (a) $M_w < M_w^{cr}$, (b) $M_w = M_w^{cr}$, (c) $M_w > M_w^{cr}$, ω^{**} is real, (d) $M_w > M_w^{cr}$, ω^{**} is pure imaginary. Continuous curves are images of $\operatorname{Im}\omega > 0$, and dashed curves are images of $\operatorname{Im}\omega < 0$. Bold curves are level lines $\operatorname{Im}\omega = 0$, $\operatorname{Re}\omega \geqslant 0$. Branches of $k(\omega)$ are marked by numbers as follows: branch $k_n(\omega)$ maps the region $\operatorname{Re}\omega > 0$, $\operatorname{Im}\omega > 0$ into the region that contains the number n. Branch points of $k(\omega)$ are shown by circles, and arrows show directions where the branch points move while M_w increases.

asymptotic behaviour of the solution is the point with the smaller $|k|$, which will be denoted by k^* as before. At this point, roots k_2 and k_3 coincide. At the other branch point, k^{**}, branches k_3 and k_4 coalesce; hence, it has no relation to the asymptotic behaviour. As the frequency ω^* corresponding to k^* is real, we conclude that for $M_w > M_w^{cr}$, instability of the plate is convective.

When M_w is further increased, one more bifurcation occurs: ω^{**} moves along the real axis towards 0, where it coincides with the branch point reflected from the imaginary axis. This bifurcation is only due to the second equation (5.12) and hence occurs only in the ω plane. After that, ω^{**} moves along the imaginary axis and stays on it for an arbitrarily large M_w. Level lines after this bifurcation are shown in figure 10(d); it is seen that at point k^{**}, the same branches k_3 and k_4 coalesce; hence, the only branch point governing instability is still k^*.
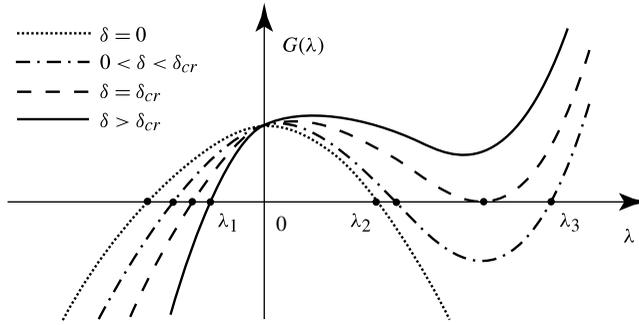
FIGURE 11. Plot $G(\lambda)$ for different values of δ.

The third branch point ω^{***} does not interact with other points for any M_w and, as before, has no relation to instability.

5.4. *Untensioned plate in flow with the boundary layer*

Let us now investigate the effect of the boundary layer and first consider the case of no plate tension: $M_w = 0$. With this assumption, the study of the branch point location is conducted analytically. Move the term with μ in (5.9) and (5.10) to the right-hand side and divide one equation by the other. In the resulting equation, k and ω are presented only in the combination $\lambda = k^2/(\mathrm{i}\omega)$:

$$D\lambda^2 = \frac{a + \delta b\lambda}{3a - 5\delta b\lambda}. \tag{5.19}$$

The equation transforms to

$$G(\lambda) = 5D\delta b\lambda^3 - 3Da\lambda^2 + \delta b\lambda + a = 0. \tag{5.20}$$

When this cubic equation is solved, ω and k are easily found. Indeed, rewrite (5.10) in the following form:

$$4\frac{\omega^2}{k} = \mu \mathrm{i}\beta(\lambda), \quad \beta(\lambda) = \frac{3a - 5\delta b\lambda}{(a - \delta b\lambda)^2}. \tag{5.21}$$

Solving the system

$$4\frac{\omega^2}{k} = \mu \mathrm{i}\beta(\lambda), \quad \frac{k^2}{\omega} = \mathrm{i}\lambda, \tag{5.22}$$

we find the branch points

$$\omega = \left(\frac{-\mathrm{i}\mu^2\lambda\beta^2(\lambda)}{16}\right)^{1/3}, \quad k = -\frac{4\mathrm{i}\omega^2}{\mu\beta(\lambda)}. \tag{5.23}$$

It is seen that each root λ of (5.20) yields three different branch points. As (5.20) has three roots λ, we have 9 different branch points in total. They all satisfy the condition $k \sim \mu^{1/3}$, $\omega \sim \mu^{2/3}$; consequently, simplifications in the dispersion relation for small μ are correct.

Consider solutions of (5.20) and choose branch points responsible for instability. It is convenient to solve (5.20) graphically. At $\delta = 0$, there are two real roots of (5.20): $\lambda_1 < 0$ and $\lambda_2 > 0$ (figure 11). Amongst frequencies ω, we are interested in those lying
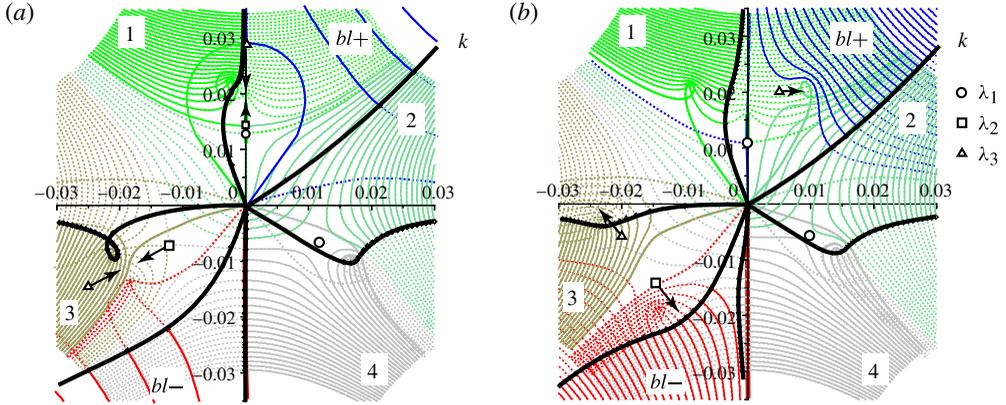
FIGURE 12. (Colour online) Level lines $\mathrm{Re}\,\omega(k) = \mathrm{const.} \geqslant 0$ in the complex k plane for parameters (5.11), $M_w = 0$: (*a*) before bifurcation, $\delta = 0.2$, (*b*) after bifurcation, $\delta = 1.2$. Continuous curves are images of $\mathrm{Im}\,\omega > 0$, and dashed curves are images of $\mathrm{Im}\,\omega < 0$. Bold curves are level lines $\mathrm{Im}\,\omega = 0$, $\mathrm{Re}\,\omega \geqslant 0$. Indices denote branches that map the quadrant $\mathrm{Re}\,\omega > 0$, $\mathrm{Im}\,\omega > 0$ into the region that contains the index. Branch points of $k(\omega)$ corresponding to λ_1, λ_2, λ_3 are represented by circles, squares, and triangles, respectively. Arrows show the direction of motion of the branch points when δ increases.

in the right half-plane. Two such frequencies correspond to the root λ_1: ω^*, which is responsible for absolute instability, and ω^{***}, which has no relation to instability. Two more frequencies correspond to λ_2: ω^{**}, whose imaginary part is negative, and ω^{***}.

For small $\delta \neq 0$, one more root $\lambda_3 > 0$ appears (figure 11) such that $\lambda_3 \sim 1/\delta$ as $\delta \to 0$. Two branch points correspond to this root: at the first, the branches k_1 and k_{bl+} coincide, while at the other, k_3 and k_{bl-} coincide. This is proved by considering level lines (figure 12*a*). It is seen that these points have no relation to instability.

Note that when the roots λ_j are real, $\beta(\lambda_j) > 0$, $j = 1, 2, 3$.

When δ increases, λ_2 increases, and λ_3 decreases such that at $\delta = \delta_{cr}$, coincidence of λ_2 and λ_3 occurs. After that, they become complex conjugate (figure 11). As an example, for parameters (5.11), $\delta_{cr} \approx 0.89$. There are no other bifurcations of λ_j, as well as no more bifurcations of ω, since $\beta(\lambda_j) \neq 0, \infty$. Thus, the only possibility for branch point bifurcation is the coincidence of λ_2 and λ_3. After this coincidence, we will assign index 2 to the root with a positive imaginary part, i.e. $\mathrm{Im}\,\lambda_2 > 0$, $\mathrm{Im}\,\lambda_3 < 0$.

Level lines after the bifurcation are shown in figure 12(*b*). In the branch point that corresponds to λ_2, branches k_4 and k_{bl-} coincide; in two other branch points that correspond to λ_3, k_3 coincides with k_4, and k_2 coincides with k_{bl+}. As before, these points have no relation to instability.

For any $\delta \geqslant 0$, the root λ_1 stays real and negative, and $\beta(\lambda_1)$ stays real and positive. Corresponding branch points do not bifurcate. We conclude that in the presence of the boundary layer, the branch point ω^*, which is responsible for the instability, keeps its imaginary part positive. Thus, we have proved that absolute instability is preserved in the presence of the boundary layer.

Let us now prove that $\mathrm{Im}\,\omega^*$ decreases monotonically when δ increases, i.e.

$$(\lambda \beta^2(\lambda))'_\delta > 0 \tag{5.24}$$

at $\lambda = \lambda_1$. It is sufficient to consider the case $D = a = b = 1$, as the general case is reduced to the latter by a linear transformation of λ and δ, which also linearly
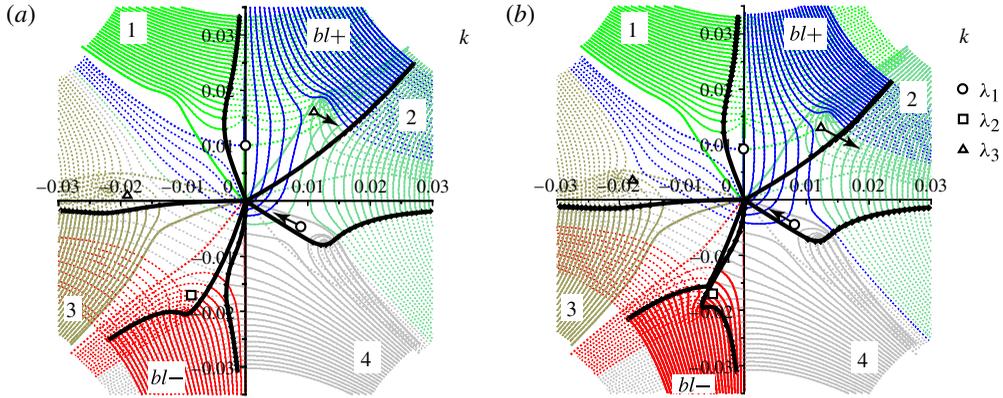
FIGURE 13. (Colour online) Level lines $\mathrm{Re}\,\omega(k) = \mathrm{const.} \geqslant 0$ in the complex k plane for parameters (5.11), $M_w = 0$: (a) before switch, $\delta = 2.2$, (b) after switch, $\delta = 3.0$. All signs are the same as in figure 12.

transforms $\beta(\lambda)$. First calculate

$$\frac{\mathrm{d}\lambda}{\mathrm{d}\delta} = -\frac{\partial G/\partial \delta}{\partial G/\partial \lambda} = -\frac{5\lambda^3 + \lambda}{15\delta\lambda^2 - 6\lambda + \delta}. \tag{5.25}$$

Next, using the definition of $\beta(\lambda)$, we obtain

$$(\lambda\beta^2(\lambda))'_\delta = \frac{3 - 5\delta\lambda}{(1 - \delta\lambda)^2}\left[\lambda'(3 - 5\delta\lambda) + \frac{2\lambda}{1 - \delta\lambda}(\delta\lambda)'(1 - 5\delta\lambda)\right]. \tag{5.26}$$

For $\lambda = \lambda_1 < 0$, the multiplier of the square brackets is positive. The first term in square brackets is positive. Also,

$$(\delta\lambda)'_\delta = \lambda + \delta\lambda' = \frac{\lambda^2(10\delta\lambda - 6)}{15\delta\lambda^2 - 6\lambda + \delta} < 0, \tag{5.27}$$

which means that the second term in square brackets is also positive. Thus, the inequality (5.24) is proved; hence, $\mathrm{Im}\,\omega^*$ decreases when δ increases. We conclude that if the plate is not tensioned, then the boundary layer decreases the growth rate of absolute instability but cannot suppress the instability (i.e. $\mathrm{Im}\,\omega^* > 0$).

When δ is increased further, k_2 and k_4 coincide in the branch point ω^* up to a certain value of δ, after which k_{bl+} substitutes k_2 so that branches k_{bl+} and k_4 coincide at this point (figure 13). This switch from k_2 to k_{bl+} occurs without bifurcation of the branch points. For parameters (5.11), this switch occurs at $\delta \approx 2.55$. At larger δ, other switches occur; however, the only important thing is that the branches that coincide at this point belong to different groups. Hence, this branch point governs absolute instability, no matter which waves generate this instability. We conclude that absolute instability, which in uniform flow was generated by the interaction of two plate waves, for large boundary layer thickness changes its form: it is generated by the interaction of boundary layer wave travelling downstream with the plate wave travelling upstream. Note that the same kind of interaction, but in incompressible fluid and with viscosity taken into account, was studied by Wiplier & Ehrenstein (2001).

5.5. *Tensioned plate, thin boundary layer*

In the absence of the boundary layer ($\delta = 0$), instability stays absolute while $M_w < M_w^{cr}$. At $M_w = M_w^{cr}$, two branch points merge such that for $M_w > M_w^{cr}$, the frequency in the branch point responsible for instability is real (i.e. the instability is convective). In the presence of the boundary layer, the system (5.9), (5.10) is too complicated for analytical investigation; that is why in this section we restrict our attention to the case of small δ, which can still be treated analytically. Linearize (5.9), (5.10) with respect to δ:

$$4Dk^3 + 2M_w^2 k - \frac{\mu}{\mathrm{i}a}\left(1 + 3\frac{\delta bk^2}{\mathrm{i}a\omega}\right) = 0, \tag{5.28a}$$

$$2M_w^2 k^2 - 4\omega^2 - \frac{3\mu k}{\mathrm{i}a}\left(1 + \frac{1}{3}\frac{\delta bk^2}{\mathrm{i}a\omega}\right) = 0. \tag{5.28b}$$

Let k_0, ω_0 be the solutions of this system at $\delta = 0$. For small δ, suppose $k = k_0 + \delta\tilde{k}$, $\omega = \omega_0 + \delta\tilde{\omega}$, substitute into (5.28), and linearize. We obtain the following:

$$12Dk_0^2\tilde{k} + 2M_w^2\tilde{k} + 3\mu\frac{b}{a^2}\frac{k_0^2}{\omega_0} = 0, \tag{5.29a}$$

$$4M_w^2 k_0\tilde{k} - 8\omega_0\tilde{\omega} - \frac{3\mu\tilde{k}}{\mathrm{i}a} + \mu\frac{b}{a^2}\frac{k_0^3}{\omega_0} = 0, \tag{5.29b}$$

which yields

$$\tilde{k} = -3\mu\frac{b}{a^2}\frac{k_0^2}{\omega_0}\frac{1}{12Dk_0^2 + 2M_w^2}, \tag{5.30a}$$

$$\tilde{\omega} = \frac{\mu}{8\omega_0}\frac{b}{a^2}\frac{k_0^2}{\omega_0}\left(-3\frac{4M_w^2 k_0 + 3\mathrm{i}\mu/a}{12Dk_0^2 + 2M_w^2} + k_0\right). \tag{5.30b}$$

An investigation of the sign of $\mathrm{Im}\,\tilde{\omega}$ is now reduced to an analysis of branch point properties at $\delta = 0$.

The only interesting case is $M_w > M_w^{cr}$, when $\mathrm{Im}\,\omega_0 = 0$, and stability is governed by the sign of $\mathrm{Im}\,\tilde{\omega}$. Note that the denominator of the fraction in parentheses in the second equality (5.30) is the derivative of the left-hand side of the first equation (5.12). At $M_w = M_w^{cr}$, when two roots of the first equation (5.12) coincide, the denominator is equal to zero. When $M_w > M_w^{cr}$, the denominator for $k_0 = k_0^*$ is positive. Now consider the numerator of the same fraction. At $M_w = M_w^{cr}$, it is also zero, whereas for $M_w > M_w^{cr}$ and $k_0 = k_0^*$, it is purely imaginary with a positive imaginary part. As $\mathrm{Im}\,k_0^* < 0$, the imaginary part of the expression in parentheses is negative. Consequently, $\mathrm{Im}\,\tilde{\omega}^* > 0$. This means that a thin boundary layer yields the shift of the frequency ω^* from the real axis to the top half-plane, i.e. $\mathrm{Im}\,\omega^* = \sigma\,\mathrm{Im}\,\tilde{\omega}^* > 0$.

Thus we have proved that for $M_w > M_w^{cr}$ a thin boundary layer converts convective instability to absolute instability.

5.6. *Tensioned plate, boundary layer of finite thickness*

In the case of finite δ, investigation of the system (5.9), (5.10) is conducted numerically. Figure 14 shows the results of calculations, namely, the location of branch points for parameters (5.11) and $0 \leqslant M_w \leqslant 0.25$ for values of $\delta = 0, 0.5, 1.0, 1.5, 2.0$ (note that for the parameters considered, $M_w^{cr} \approx 0.13$). It is seen that the point ω^* stays in the upper half-plane for all δ analysed. The topology of level lines in figure 15
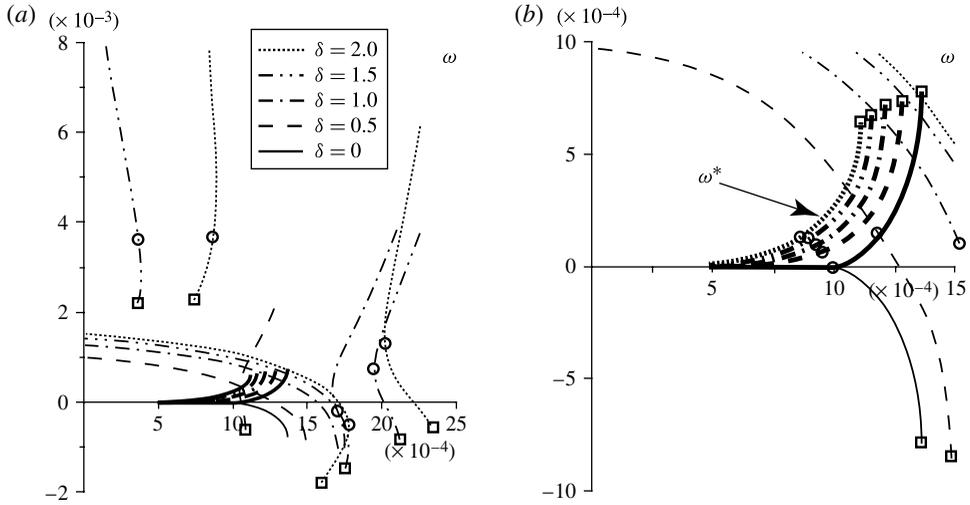
FIGURE 14. (*a*) Traces of the branch points in the ω plane for parameters (5.11) and $0 \leqslant M_w \leqslant 0.25$, $\delta = 0, 0.5, 1.0, 1.5, 2.0$. (*b*) Close-up of the area of small ω. Bold curves represent the frequency ω^*. Values at $M_w = 0$ are represented by squares, and values at $M_w = M_w^{cr} \approx 0.13$ are represented by circles.
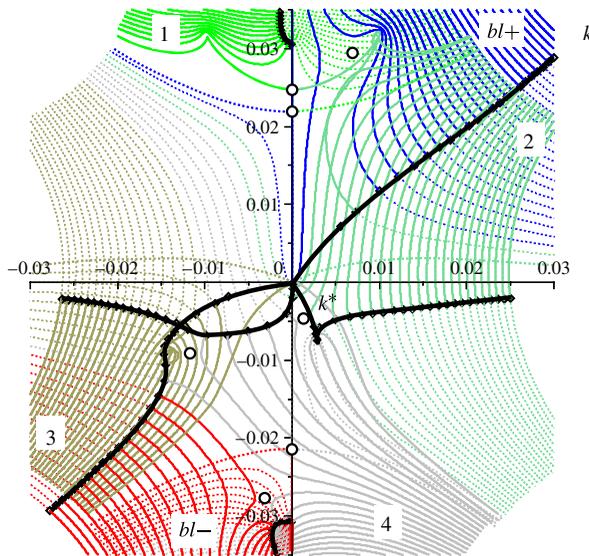

FIGURE 15. (Colour online) Level lines $\operatorname{Re}\omega(k) = \text{const.} \geqslant 0$ in the complex k plane for parameters (5.11), $M_w = 0.15$, $\delta = 1.5$. All signs are the same as in figure 12.

shows that this is the only branch point where roots from different groups coincide. No branch point bifurcation was detected in the range of parameters analysed.

Thus, absolute instability generated by the boundary layer for infinitesimal δ is preserved for finite values of δ from the range of parameters studied.
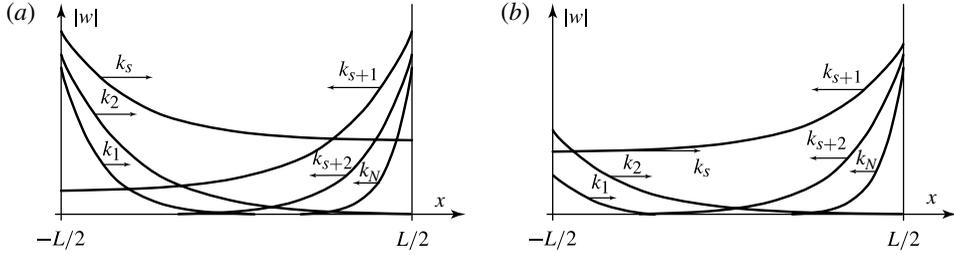
FIGURE 16. Ordering spatial waves (*a*) for $\mathrm{Im}\,\omega \to +\infty$, (*b*) for ω obeying (6.2).

6. Flutter of finite plates

6.1. *Global instability criterion*

In this section, we investigate the influence of the boundary layer on flutter of a large but finite plate. The stability criterion of a finite plate (no matter how long it is) is generally different from the criterion for an infinite plate, and was derived in a general form by Kulikovskii (1966*a*).

In order to formulate this criterion and explain its physical nature, let us first number the roots of the dispersion relation for infinite plate $k_j(\omega)$ in the order of decrease of $\mathrm{Im}\,k_j(\omega)$ for $\mathrm{Im}\,\omega \gg 1$. Then all roots are split into two groups in the same manner as in § 5.1: the first consists of such roots that $\mathrm{Im}\,k_j(\omega) > 0$ as $\mathrm{Im}\,\omega \to +\infty$, $j = 1, \ldots, s$; the second consists of roots with $\mathrm{Im}\,k_j(\omega) < 0$ as $\mathrm{Im}\,\omega \to +\infty$, $j = s+1, \ldots, N$. From a physical point of view, the first group represents waves travelling from left to right (downstream), and waves from the second group travel from right to left (upstream), as shown in figure 16(*a*). For downstream-travelling waves, an increase of j corresponds to a decrease of the spatial damping of the wave. The least damped downstream-travelling wave, therefore, corresponds to the wavenumber k_s. In contrast, for upstream-travelling waves, an increase of j corresponds to an increase of the spatial damping; the least damped upstream-travelling wave has the wavenumber k_{s+1}. When $\mathrm{Im}\,\omega$ decreases, branches k_j are analytically continued, keeping their numbering, from the region of $\mathrm{Im}\,\omega \to +\infty$. For sufficiently small $\mathrm{Im}\,\omega$ values, $\mathrm{Im}\,k_j(\omega)$ can change signs; in this case, the wave becomes spatially amplified. Its apparent behaviour becomes deceptive: downstream-travelling waves can become amplified in the downstream direction. That is why it is important to order wavenumbers and classify them as downstream-travelling and upstream-travelling as $\mathrm{Im}\,\omega \to +\infty$, when there are no doubts about the travelling direction and spatial behaviour of the waves.

Kulikovskii (1966*a*) considered eigenmodes of a finite-length system in the form of a linear combination of waves travelling in an infinite system, which satisfies the boundary conditions at the boundaries of the finite system. Namely, the substitution of

$$w(x, t) = \sum_{j=1}^{N} C_j \mathrm{e}^{\mathrm{i}(k_j(\omega)x - \omega t)} \tag{6.1}$$

into boundary conditions at $x = \pm L/2$ (where L is the plate length) yields the frequency equation. He proved that the asymptotic form of the latter as $L \to \infty$ is as follows:

$$\min_{j=1,\ldots,s}\,\mathrm{Im}\,k_j(\omega) = \max_{j=s+1,\ldots,N}\,\mathrm{Im}\,k_j(\omega). \tag{6.2}$$

In other words, solutions of this equation form a limit set of eigenvalues as $L \to \infty$. This equation does not depend on the boundary conditions assigned at the plate edges (indeed, it contains only roots of the dispersion relation for an infinite plate). Its solutions form a curve Ω in the complex ω plane, such that eigenvalues of the finite plate in the gas flow are concentrated near this curve. If there is a piece of this curve lying in the region $\mathrm{Im}\,\omega > 0$, then the plate of a sufficiently long length is unstable, because there exists an eigenfrequency located in the neighbourhood of this piece of Ω. The system is then called globally unstable.

Equation (6.2) and eigenmodes corresponding to its solutions have a clear physical representation. Imagine that at the leading edge of the plate ($x = -L/2$), a wave with the wavenumber k_s travelling downstream is generated. When it comes to the trailing edge ($x = L/2$), it is reflected and transformed into upstream-travelling waves corresponding to $k_{s+1} \ldots k_N$. Amongst these waves, the least damped wave corresponds to k_{s+1}, so that when they approach the leading edge, for a sufficiently long plate length L, we can neglect all other waves as their amplitudes are negligible in comparison with the wave with k_{s+1}. The latter is reflected from the leading edge and transforms into waves travelling downstream with $k_1 \ldots k_s$. When they approach the trailing edge, the amplitudes of those with wavenumbers $k_1 \ldots k_{s-1}$ for sufficiently large L are negligible so that the only essential wave corresponds to k_s. As the frequency ω satisfies (6.2), the amplitude of the initially generated wave with k_s remains the same after the double reflection, i.e. we have exactly the same state as two reflections before. This process of reflections is cyclically continued, representing the finite plate eigenmode.

Kulikovskii's criterion (6.2) has been successfully used in various applications: stability of the Poiseuille flow in a finite-length pipe (Kulikovskii 1966*b*, 1968), vibrations of a fluid-conveying pipe (Kulikovskii & Shikina 1988), stability of an elastic plate in a flow of incompressible fluid (Peake 2004), and other problems (Doaré & de Langre 2006).

Evidently, if the infinite system is absolutely unstable (i.e. $k_p(\omega) = k_q(\omega)$, $p \in 1 \ldots s$, $q \in s + 1 \ldots N$ for some ω, $\mathrm{Im}\,\omega > 0$), then the finite system is globally unstable, since (6.2) is satisfied. The inverse statement is generally not correct.

Let us now apply criterion (6.2) to the problem under consideration. An investigation at $\delta = 0$ (uniform flow) was conducted by Vedeneev (2005). In this case, there are four roots of (3.6): k_1 and k_2 form the first group, k_3 and k_4 the second. If the plate tension is sufficiently small that $M_w < M_w^{cr}$, then curve Ω consists of two parts shown in figure 17(*a*). The first one, Ω_1, is defined by the equation $\mathrm{Im}\,k_1(\omega) < \mathrm{Im}\,k_2(\omega) = \mathrm{Im}\,k_3(\omega) < \mathrm{Im}\,k_4(\omega)$ and corresponds to single-mode flutter of the finite plate. The second part, Ω_2, is defined by the equation $\mathrm{Im}\,k_1(\omega) < \mathrm{Im}\,k_2(\omega) = \mathrm{Im}\,k_4(\omega) < \mathrm{Im}\,k_3(\omega)$ and corresponds to coupled-mode flutter. The curve Ω_2 ends in the branch point $k_2(\omega^*) = k_4(\omega^*)$, where points of Ω_2 achieve the maximum of $\mathrm{Im}\,\omega$. This branch point also yields an absolute instability of an infinite plate. If the plate tension is sufficiently large that $M_w > M_w^{cr}$, then coupled-mode flutter is suppressed, Ω_2 is not present, and Ω_1 (figure 17*b*) ends in the branch point $k_2(\omega^*) = k_3(\omega^*)$ (figures 10*c* and 10*d*).

6.2. *Coupled-mode flutter*

In §5, we have proved that an infinite plate is always absolutely unstable in the presence of the boundary layer. Therefore, a finite plate of a sufficiently long length is also unstable.
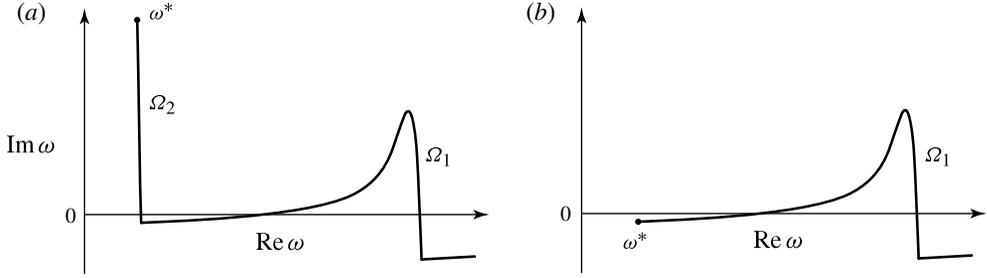
FIGURE 17. Typical shape of the curve Ω for (*a*) both single-mode and coupled-mode flutter, (*b*) single-mode flutter only.
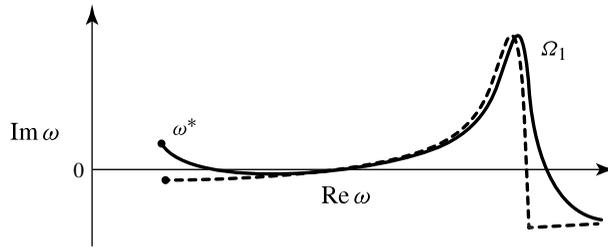

FIGURE 18. Shift of ω^* and resulting shape of the curve Ω for single-mode flutter in uniform flow (dashed) and in the presence of the boundary layer (continuous).

For $M_w < M_w^{cr}$, the branch point ω^* that yields to instability is formed by the merging of branches k_2 and k_4. By definition, this case is referred to as coupled-mode flutter; hence, we conclude that coupled-mode flutter, if present in uniform flow, is retained in the presence of the boundary layer, although the growth rate is decreased.

For $M_w > M_w^{cr}$, the branch point ω^* is formed by the merging of branches k_2 and k_3, which is referred to as single-mode flutter. In uniform flow $\mathrm{Im}\,\omega^* < 0$ (figure 17*b*); consequently, this branch point does not yield instability (in §5.3, we claimed that $\mathrm{Im}\,\omega^* = 0$; actually, ω^* is slightly shifted to the bottom half-plane due to terms that were neglected when we simplified the dispersion relation). However, as shown in §§5.5 and 5.6, the boundary layer yields shift of ω^* to the upper half-plane. Thus the end of Ω_1 is shifted into the upper half-plane by the boundary layer (figure 18). Note that this shift occurs no matter what velocity and temperature profiles the boundary layer has. In contrast, in §6.3 below, we will show that the change of Ω_1 shape in the region $|\omega| \gg \mu^{2/3}$, especially around the hump, depends on the boundary layer profiles.

6.3. *Single-mode flutter*

According to Vedeneev (2005), in uniform flow ($\delta = 0$), the curve Ω in the region $|\omega| \gg \mu^{2/3}$ is defined by the equation $\mathrm{Im}\,k_2(\omega) = \mathrm{Im}\,k_3(\omega)$, where k_2 and k_3 are branches of the solution of the dispersion equation for an infinite plate (3.6) that correspond to waves travelling downstream (k_2) and upstream (k_3). Now let $\delta \neq 0$. As μ is a small parameter, we assume $\omega = \omega_R + \mathrm{i}\omega_I$, $|\omega_I| \ll 1$ and obtain the Taylor expansion

$$k_j(\omega_R + \mathrm{i}\omega_I, \mu) = k_j(\omega_R, 0) + \mathrm{i}\frac{\omega_I}{g_j} + \mu\Delta(k_j) + o(\omega_I, \mu), \qquad (6.3)$$

where

$$\Delta(k_j) = \frac{1}{2k_j(M_w^2 + 2Dk_j^2)} \left(\left(\frac{(M_\infty k_j - \omega)^2}{\sqrt{k_j^2 - (M_\infty k_j - \omega)^2}} \right)^{-1} \right.$$

$$\left. + \delta \left(\int_0^1 \frac{T_0(\eta)\,d\eta}{(u_0(\eta) - c_j)^2} - 1 \right) \right)^{-1}, \tag{6.4}$$

$c_j = \omega_R/k_j$ is a phase velocity, and $g_j = d\omega_R/dk_j$ is a group velocity. Denoting

$$g(\omega) = g_2 = -g_3 = \frac{2Dk_2^3 + k_2 M_w^2}{\omega}, \tag{6.5}$$

we obtain the equation for curve Ω_1

$$\omega_I = -\frac{\mu g(\omega_R)}{2} \text{Im}(\Delta(k_2(\omega_R)) - \Delta(k_3(\omega_R)))$$

$$= -\frac{\mu}{2\omega_R} \text{Im} \left((A + B)_2^{-1} + (A + B)_3^{-1} \right), \tag{6.6}$$

where A and B are defined in § 4 for each single wave.

Thus, the growth rate of the finite plate eigenmode is the arithmetic mean of growth rates of downstream-travelling and upstream-travelling waves.

As well as for an infinite plate (§§ 4.1 and 4.4), we will consider three types of eigenmodes distinguished by the behaviour of downstream-travelling waves in uniform flow: growing, neutral, or damped. Consider the first case. If the boundary layer profile is generalized convex, then the downstream-travelling wave stays growing, but its growth rate is decreased in comparison with the uniform flow. A damped wave travelling upstream stays damped, but its damping rate is also decreased in comparison with the uniform flow. The total growth rate of the eigenmode, equal to the arithmetic mean of the growth rates, generally speaking, can lead to a change in the growth rate by the boundary layer both to larger and smaller values. For typical boundary layer profiles, calculations show that the total growth rate decreases or even becomes negative (i.e. the eigenmode is damped); see § 6.4 below for details.

If the boundary layer profile has a generalized inflection point such that $(u_0'/T_0)' > 0$ for $0 < z < z_{infl}$, then there is a range of phase velocities c of the downstream-travelling wave such that $\text{Im}\,B < 0$. For such values of c, the growth rate of the downstream-travelling wave is increased for $\delta < \delta_1$. Since the damping rate of the upstream-travelling wave is decreased, we conclude that the total growth rate of the finite plate eigenmode is increased by the boundary layer. This effect is typical for decelerating flow profiles, where the amplification of the downstream-travelling wave can be large (§ 4.2).

Now consider the second type of eigenmodes, which corresponds to neutral downstream-travelling waves. Eigenmodes that correspond to $c \in [M_\infty; M_\infty + 1]$ are damped as the downstream-travelling wave is neutral and the upstream-travelling wave is damped. The behaviour of those corresponding to $c \in [M_\infty - 1; M_\infty]$ depends on the boundary layer. Let the boundary layer profile be generalized convex or have a generalized inflection point in the supersonic part of the layer (i.e. $(u_0'/T_0)' < 0$ in the subsonic part of the layer $z > z_s$, where z_s is the sonic point, $u_0(z_s) = M_\infty - 1$). Then for phase velocities close to $M_\infty - 1$, the growth rate of the downstream-travelling wave is increased by the boundary layer, which can be sufficient to exceed the damping rate
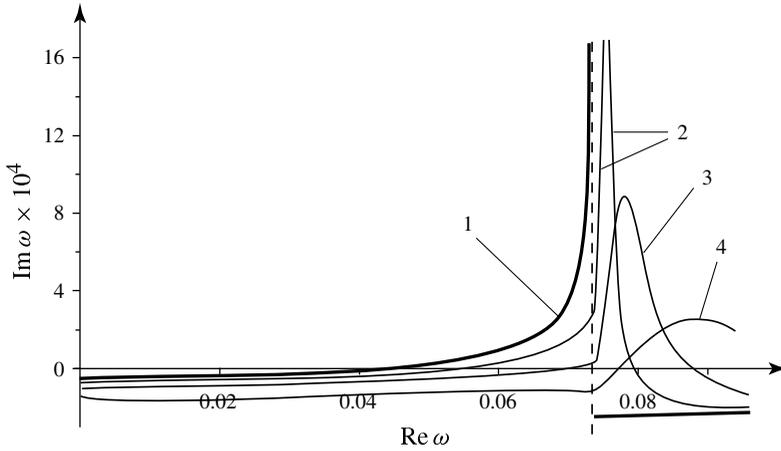
FIGURE 19. Curve Ω_1 for profile 1 in figure 5. Vertical dashed line corresponds to the sonic eigenmode (i.e. phase speed of the wave travelling downstream $c = M_\infty - 1$). Curves 1–4: $\delta = 0, 0.5, 1, 2$, respectively.

of the upstream-travelling wave. The total action on the eigenmode in this case is the growth of the finite plate eigenmode.

If the boundary layer profile has a generalized inflection point in the subsonic part of the layer, which is located far enough from the sonic point z_s (i.e. there is a sufficiently wide segment $z_s < z < z_{infl}$, where $(u'_0/T_0)' > 0$), then the growth rate of the downstream-travelling wave is small and does not exceed the damping rate of the upstream-travelling wave. The total action is the damping of the finite plate eigenmode.

For the third type of eigenmodes, both downstream-travelling and upstream-travelling waves are damped, and finite plate eigenmodes are also damped.

6.4. *Examples*

Let us summarize the results obtained in the previous section. We will call an eigenmode supersonic or subsonic if its downstream-travelling wave is supersonic or subsonic relating to the flow, respectively (i.e. $0 < c < M_\infty - 1$ or $M_\infty - 1 < c < M_\infty$, respectively). Then for a generalized convex profile of the boundary layer, growth rates of supersonic plate eigenmodes are decreased, while the growth rates of subsonic eigenmodes are increased in comparison with the uniform flow. For the profile with a generalized inflection point in the subsonic part of the layer, located far from the sonic point, the growth rate of supersonic eigenmodes is larger than in the uniform flow for $\delta < \delta_1$; supersonic eigenmodes are damped for $\delta > \delta_2$, and subsonic eigenmodes are damped for any δ.

For example, consider a generalized convex profile of accelerating flow, which corresponds to $\beta = 2.0$ (profile 1 in figure 5). The calculated curve Ω_1 is shown in figure 19. It is seen that while increasing the boundary layer thickness δ, Im ω for supersonic eigenmodes decreases and becomes negative. At the same time, subsonic eigenmodes are destabilized by the boundary layer.

Now consider decelerating flow, which corresponds to $\beta = -0.199$ (profile 5 in figure 5). Shown in figure 20 is the calculated curve Ω_1. For $\delta < \delta_1$, the instability of supersonic modes becomes stronger: Im ω for growing eigenmodes increases, while
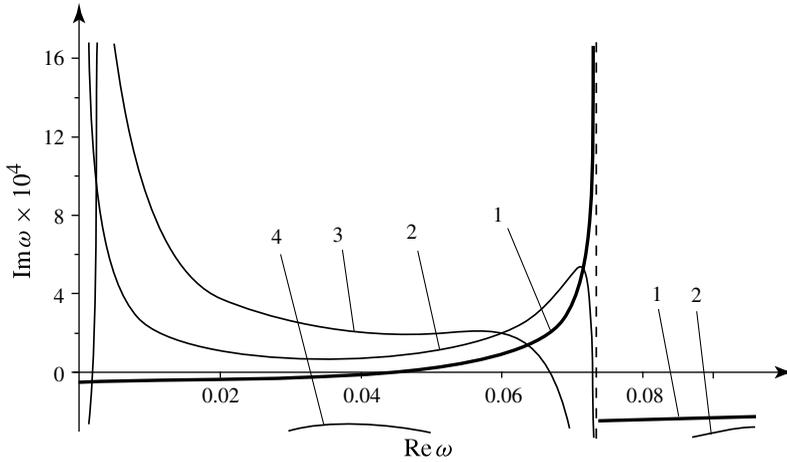
FIGURE 20. Curve Ω_1 for profile 5 in figure 5. Vertical dashed line corresponds to the sonic eigenmode (i.e. phase speed of the wave travelling downstream $c = M_\infty - 1$). Curves 1–4: $\delta = 0, 0.5, 1, 2$, respectively.

damped eigenmodes grow. For $\delta > \delta_2$ (curve 4 in figure 20), supersonic eigenmodes are all damped. Subsonic eigenmodes stay damped as the flow speed at generalized inflection point $u_0(z_{infl}) \approx 1.07 > M_\infty - 1$.

7. Conclusions

In this paper, the influence of the boundary layer over an elastic plate on the stability of infinite-length and finite-length plates has been investigated.

In the case of a generalized convex boundary layer profile, which is typical for accelerating flows, supersonic plate waves (in an infinite plate) or eigenmodes in single-mode flutter (in a finite-length plate) are stabilized, and subsonic waves are destabilized. In the case of the boundary layer profile with a generalized inflection point located in the subsonic (relative to the flow) part of the layer (typical for constant and decelerating mean flow), supersonic perturbations are destabilized if $\delta < \delta_1$ and stabilized if $\delta > \delta_2$. Subsonic perturbations are damped.

The relation between the influence of the boundary layer on plate stability and the stability of the boundary layer over a rigid wall has been studied. An example has been given of a stable boundary layer which makes the growth rate of the plate disturbances arbitrarily high.

An absolute instability of an infinite plate and the coupled-mode flutter of a finite-length plate have been studied. In the case of no pre-existing tension, the plate stays absolutely unstable (coupled-mode flutter is preserved), but the growth rate decreases when the boundary layer thickness increases. At a certain δ, a switch of waves responsible for instability occurs: in a thin boundary layer (as well as in uniform flow), it is generated by the interaction of upstream-travelling and downstream-travelling plate waves, while in a thick boundary layer, an upstream-travelling plate wave interacts with a downstream-travelling boundary layer wave.

In the case of sufficiently large plate tension, when instability of the plate in uniform flow becomes convective (the coupled-mode flutter of the finite plate disappears), the boundary layer yields absolute instability, irrespective of the velocity and temperature profiles of the boundary layer.

Acknowledgement

REFERENCES

BERS, A. 1983 Space–time evolution of plasma instabilities: absolute and convective. In *Handbook of Plasma Physics* (ed. A. A. Galeev & R. N. Sudan), chap. 3.2, pp. 451–517. North-Holland.

BOIKO, A. V. & KULIK, V. M. 2012 Stability of flat plate boundary layer over monolithic viscoelastic coatings. *Dokl. Phys.* **57** (7), 285–287.

BOLOTIN, V. V. 1963 *Nonconservative Problems of the Theory of Elastic Stability*. Pergamon Press.

BRIGGS, R. J. 1964 *Electron-Stream Interaction with Plasmas*. MIT Press.

CARPENTER, P. W. & GARRAD, A. D. 1985 The hydrodynamic stability of flow over Kramer-type compliant surfaces. Part 1. Tollmien–Schlichting instabilities. *J. Fluid Mech.* **155**, 465–510.

CARPENTER, P. W. & GARRAD, A. D. 1986 The hydrodynamic stability of flow over Kramer-type compliant surfaces. Part 2. Flow-induced surface instabilities. *J. Fluid Mech.* **170**, 199–232.

CHOMAZ, J.-M. 2005 Global instabilities in spatially developing flows: non-normality and nonlinearity. *Annu. Rev. Fluid Mech.* **37**, 357–392.

DOARÉ, O. & DE LANGRE, E. 2006 The role of boundary conditions in the instability of one-dimensional systems. *Eur. J. Mech.* B **25** (6), 948–959.

DOWELL, E. H. 1971 Generalized aerodynamic forces on a flexible plate undergoing transient motion in a shear flow with an application to panel flutter. *AIAA J.* **9** (5), 834–841.

DOWELL, E. H. 1973 Aerodynamic boundary layer effect on flutter and damping of plates. *J. Aircraft* **10** (12), 734–738.

DOWELL, E. H. 1974 *Aeroelasticity of Plates and Shells*. Noordhoff International.

DRAZIN, P. G. & REID, W. H. 2004 *Hydrodynamic Stability*. Cambridge University Press.

GAPONOV, S. A. & MASLOV, A. A. 1980 Development of perturbations in compressible flows (in Russian). Nauka.

GASPERS, P. A. Jr, MUHLSTEIN, L. Jr & PETROFF, D. N. 1970 Further results on the influence of the turbulent boundary layer on panel flutter. NASA TN D-5798.

HASHIMOTO, A., AOYAMA, T. & NAKAMURA, Y. 2009 Effect of turbulent boundary layer on panel flutter. *AIAA J.* **47** (12), 2785–2791.

HUERRE, P. & MONKEWITZ, P. A. 1985 Absolute and convective instabilities in free shear layers. *J. Fluid Mech.* **159**, 151–168.

HUERRE, P. & MONKEWITZ, P. A. 1990 Local and global instabilities in spatially developing flows. *Annu. Rev. Fluid Mech.* **22**, 473–537.

HUNT, R. E. & CRIGHTON, D. G. 1991 Instability of flow in spatially developing media. *Proc. R. Soc. Lond.* A **435**, 109–128.

KORNECKI, A. 1979 Aeroelastic and hydroelastic instabilities of infinitely long plates. Part 2. *Solid Mech. Archives* **4** (4), 241–346.

KRAMER, M. O. 1960 Boundary layer stabilization by distributed damping. *J. Am. Soc. Nav. Engrs* **72**, 25.

KULIKOVSKII, A. G. 1966*a* On the stability of homogeneous states. *J. Appl. Math. Mech.* **30** (1), 180–187.

KULIKOVSKII, A. G. 1966*b* On the stability of Poiseuille flow and certain other plane-parallel flows in a flat pipe of large but finite length for large Reynolds numbers. *J. Appl. Math. Mech.* **30** (5), 975–989.

KULIKOVSKII, A. G. 1968 Stability of flows of a weakly compressible fluid in a plane pipe of large, but finite length. *J. Appl. Math. Mech.* **32** (1), 100–102.

KULIKOVSKII, A. G. 2006 The global instability of uniform flows in non-one-dimensional regions. *J. Appl. Math. Mech.* **70** (2), 229–234.

KULIKOVSKII, A. G. & SHIKINA, I. S. 1988 On bending vibrations of a long tube with moving fluid (in Russian). *Mechanics. Proc. Natl Acad. Sci. Armenia* **41**(1), 31–39.

LEES, L. & LIN, C. C. 1946 Investigation of the stability of the laminar boundary layer in a compressible fluid. NACA TN 1115.

LEES, L. & RESHOTKO, E. 1962 Stability of the compressible laminar boundary layer. *J. Fluid Mech.* **12**, 555–590.

LE DIZÈS, S., HUERRE, P., CHOMAZ, J. M. & MONKEWITZ, P. A. 1996 Linear global modes in spatially developing media. *Phil. Trans. R. Soc. Lond.* A **354**, 169–212.

LIN, C. C. 1966 *The Theory of Hydrodynamic Stability*. Cambridge University Press.

LINGWOOD, R. J. & PEAKE, N. 1999 On the causal behaviour of flow over an elastic wall. *J. Fluid Mech.* **396**, 319–344.

MILES, J. W. 1959 On panel flutter in the presence of a boundary layer. *J. Aerosp. Sci.* **26** (2), 81–93, 107.

MILES, J. 2001 Stability of inviscid shear flow over a flexible boundary. *J. Fluid Mech.* **434**, 371–378.

MUHLSTEIN, L. Jr, GASPERS, P. A. Jr & RIDDLE, D. W. 1968 An experimental study of the influence of the turbulent boundary layer on panel flutter. NASA TN D-4486.

PEAKE, N. 2004 On the unsteady motion of a long fluid-loaded elastic plate with mean flow. *J. Fluid Mech.* **507**, 335–366.

PIER, B., HUERRE, P. & CHOMAZ, J.-M. 2001 Bifurcation to fully nonlinear synchronized structures in slowly varying media. *Physica* D **148**, 49–96.

REUTOV, V. P. & RYBUSHKINA, G. V. 1998 Hydroelastic instability threshold in a turbulent boundary layer over a compliant coating. *Phys. Fluids* **10** (2), 417–425.

SAVENKOV, I. V. 1995 The suppression of the growth of nonlinear wave packets by the elasticity of the surface around which flow occurs. *Comput. Math. Math. Phys.* **35** (1), 73–79.

SCHLICHTING, H. 1960 *Boundary Layer Theory*. McGraw-Hill.

VEDENEEV, V. V. 2005 Flutter of a wide strip plate in a supersonic gas flow. *Fluid Dyn.* **5**, 805–817.

VEDENEEV, V. V. 2006 High-frequency plate flutter. *Fluid Dyn.* **2**, 313–321.

VEDENEEV, V. V. 2012 Panel flutter at low supersonic speeds. *J. Fluids Struct.* **29**, 79–96.

VEDENEEV, V. V., GUVERNYUK, S. V., ZUBKOV, A. F. & KOLOTNIKOV, M. E. 2010 Experimental observation of single mode panel flutter in supersonic gas flow. *J. Fluids Struct.* **26**, 764–779.

WHITHAM, G. B. 1974 *Linear and Nonlinear Waves*. Wiley.

WIPLIER, O. & EHRENSTEIN, U. 2001 On the absolute instability in a boundary-layer flow with compliant coatings. *Eur. J. Mech.* B **20** (1), 127–144.